Recent developments in the nuclear shell model and their interest for astrophysics

Kamila Sieja

Institut Pluridisciplinaire Hubert Curien, Strasbourg

Atomic nucleus: a complex object

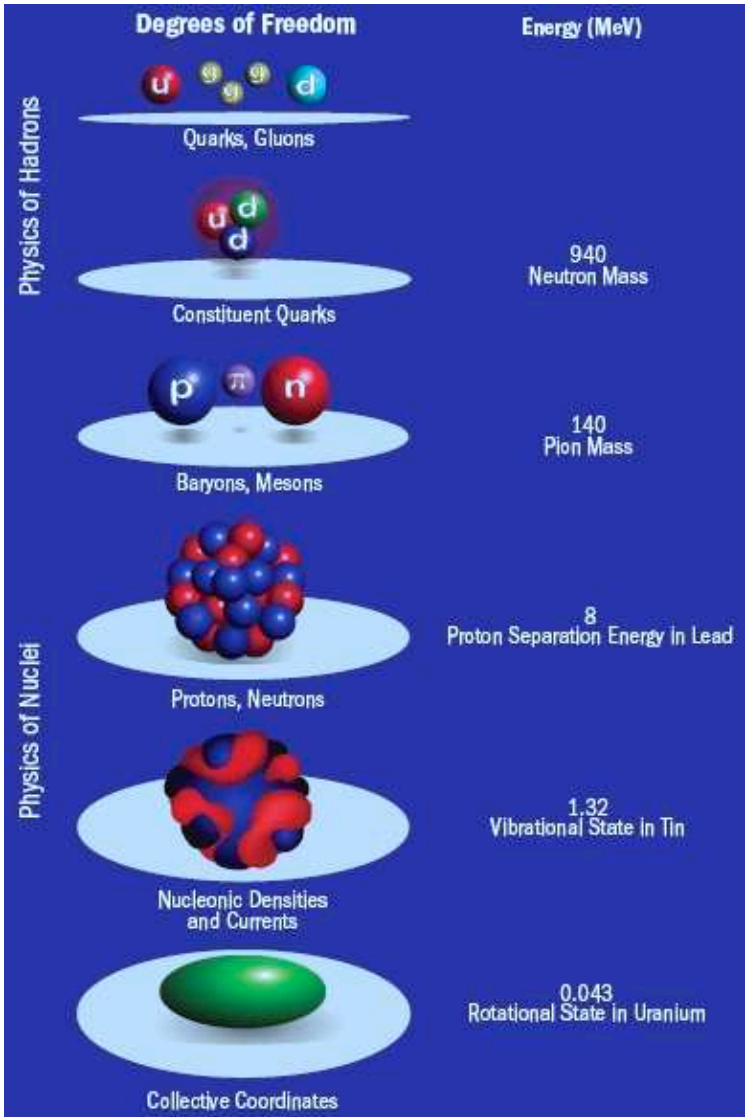

- Nucleus is a quantum object composed of neutrons and protons, which themselves are composite structures, composed of quarks and gluons. In low energy nuclear physics, the QCD degrees of freedom are not excited, but are manifested in **a very complex internucleon force**.
- In addition to the strong interaction in nuclear physics we have to deal with electromagnetic forces between positively charged protons and with weak interactions, **which is already 3 out of the 4 fundamental forces in nature !**
- Despite of the complexity of this many-body system itself and the interactions involved, the empirical knowledge shows that **surprisingly simple structures and collective phenomena occur in nuclei**.

Nuclear many-body problem

The number of nucleons in nuclei is too large for an exact solution of A-body Schrödinger equation. Still, it is much too small for statistical methods.

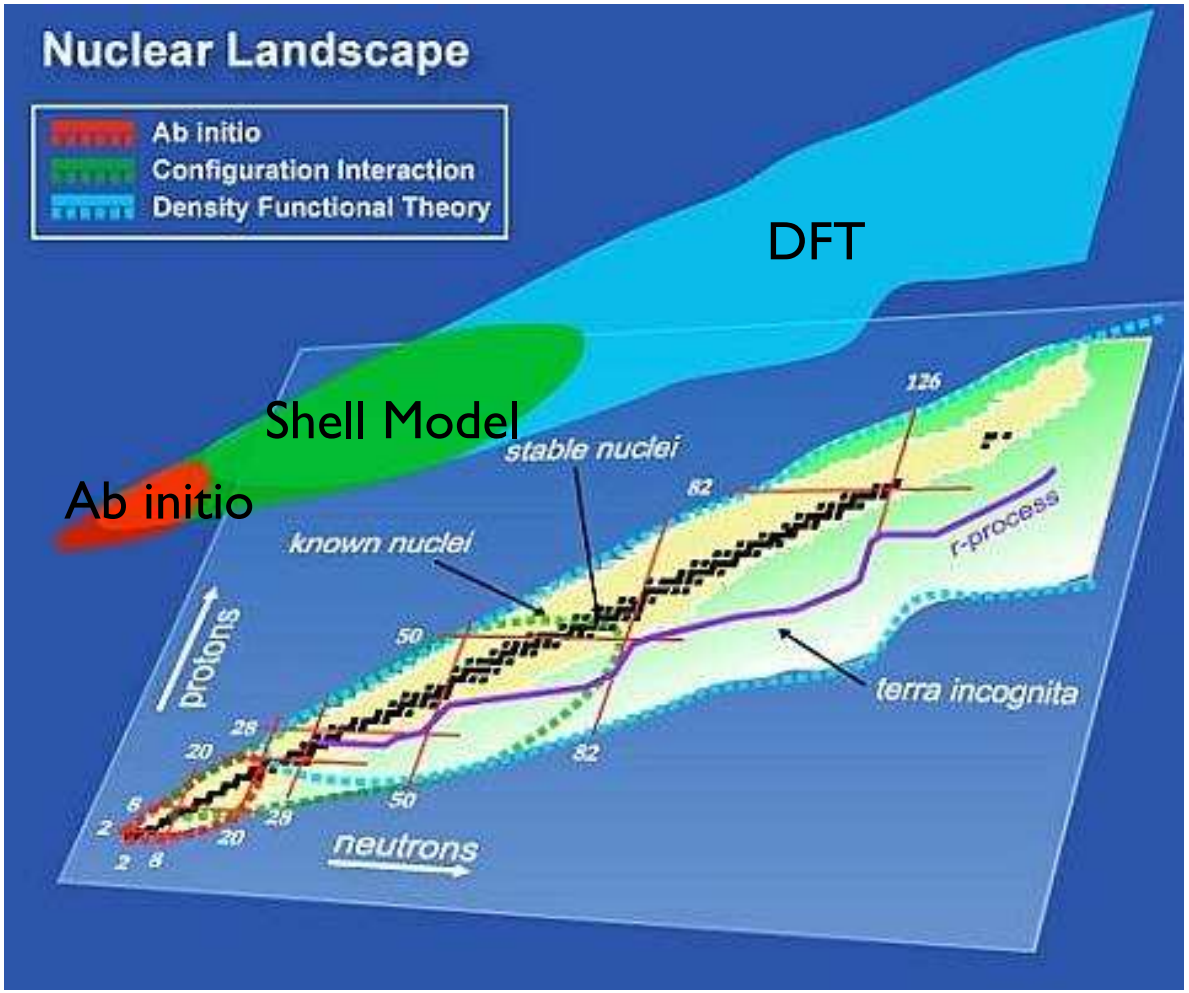

- Nuclear Shell Model (SM), known as well as Configuration Interaction (CI)
- Density Functional Theory (DFT):

$$E = \frac{\langle \Psi | H | \Psi \rangle}{\langle \Psi | \Psi \rangle} \Longleftrightarrow \mathscr{E}_{EDF}[\rho]$$

$$\rho_{ij} = \langle \phi | a_j^\dagger a_i^\dagger | \phi \rangle \Longleftarrow |\phi\rangle = \prod a_i^\dagger |-\rangle.$$

- Macroscopic-microscopic models

Shell model approach

Calculations Ab Initio

- Realistic NN interactions
- Diagonalization in $N\hbar\omega$ h.o.space

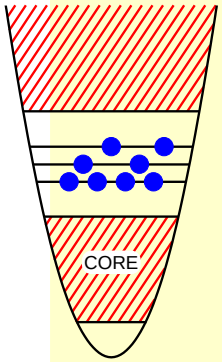

- define valence space
- $H_{\text{eff}}\Psi_{\text{eff}} = E\Psi_{\text{eff}}$

$\rightsquigarrow$ INTERACTIONS

- build and diagonalize Hamiltonian matrix

$\rightsquigarrow$ CODES

Weak processes:
- β decays
- $\beta\beta$ decays

$[T^{0\nu}_{1/2}(0^+ \rightarrow 0^+)]^{-1} = G_{0\nu}|M^{0\nu}|^2\langle m_\nu\rangle^2$

☞ASTROPHYSICS

☞PARTICLE PHYSICS

Collective excitations:
- deformation, superdeformation
- superfluidity
- symmetries

Shell evolution far from stability:
- Shell quenching
- New magic numbers

☞ASTROPHYSICS

Model spaces

- Classical $0\hbar\omega$ model spaces (e.g. *sd*-shell, *pf*-shell) are successfull for the description of a low lying states of nuclei, their transition rates and weak-decays.

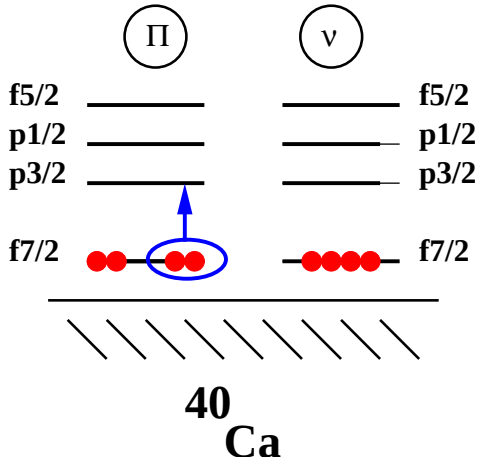

- Neutron rich nuclei require different active proton and neutron shells (e.g. *sd*-shell for protons, *pf*-shell for neutrons).

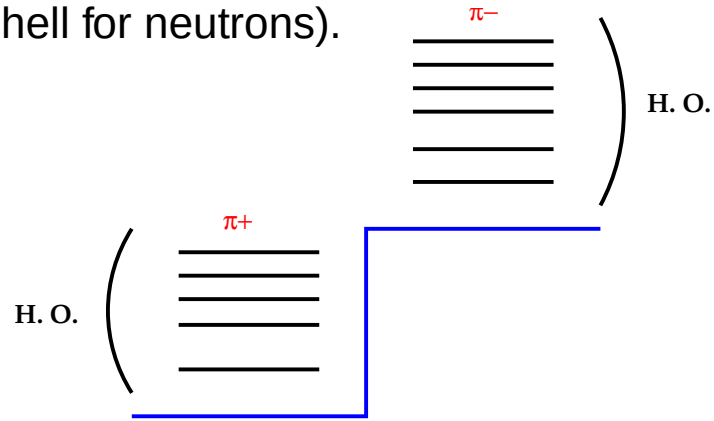

- Deformed nuclei and deformed bands in spherical nuclei are due to many-particle many-hole excitations across the gaps. At least $2\hbar\omega$ spaces are necessary e.g. *sd*-*pf* for both neutrons and protons).

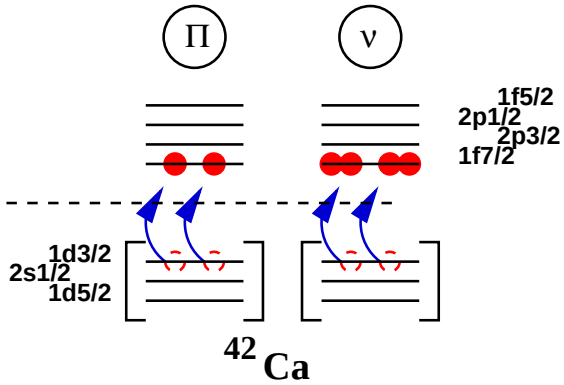

- In simple shell-model nuclei, certain observables require going beyond $0\hbar\omega$ model space, e.g. parity changing transitions.

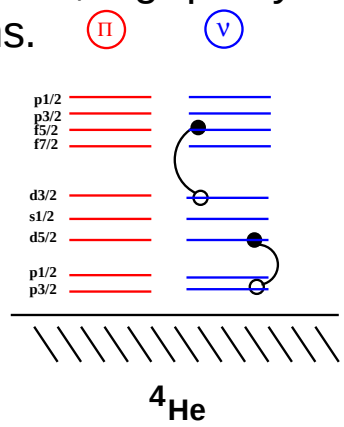

Model spaces

- Classical $0\hbar\omega$ model spaces (e.g. *sd*-shell, *pf*-shell) are successfull for the description of a large number of nuclei, their transition rates and weak-decays.

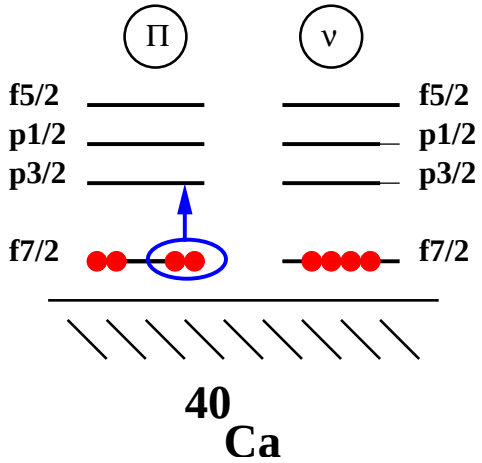

- Neutron rich nuclei require different active proton and neutron shells (e.g. *sd*-shell for protons, *pf*-shell for neutrons).

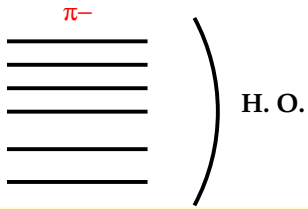

- Deformed nuclei and deformed bands in spherical nuclei are due to many-particle many-hole excitations across the gaps. At least $2\hbar\omega$ spaces are necessary e.g. $sd-pf$ for both neutrons and protons).

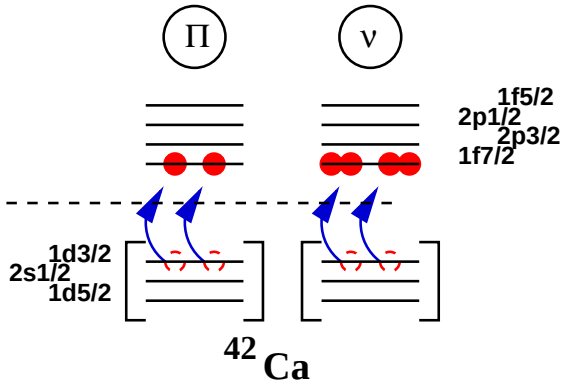

- In simple shell-model nuclei, certain observables alos require going beyond $0\hbar\omega$ model space, e.g. parity changing transitions.

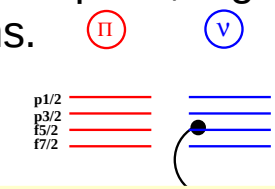

For each model space an effective SM interaction has to be constructed

^{4}He

Shell Model: giant computations

- Problem dimension in the m-scheme:

$$D \sim \begin{pmatrix} d_\pi \\ p \end{pmatrix} \cdot \begin{pmatrix} d_\nu \\ n \end{pmatrix}$$

In the *pf*-shell ($1f_{7/2}$, $2p_{3/2}$, $1f_{5/2}$, $2p_{1/2}$):

^{48}Cr 1,963,461
^{56}Ni 1,087,455,228

- Current diagonalization limit in m-scheme 10^{10}

- The largest SM diagonalization up to date has been achieved by the Strasbourg group (using very modest computing resources):
Phys. Rev. C82 (2010) 054301, ibidem 064304

  - m scheme CODE ANTOINE
  - coupled scheme CODE NATHAN

E. Caurier et al., Rev. Mod. Phys. 77 (2005) 427;
ANTOINE website

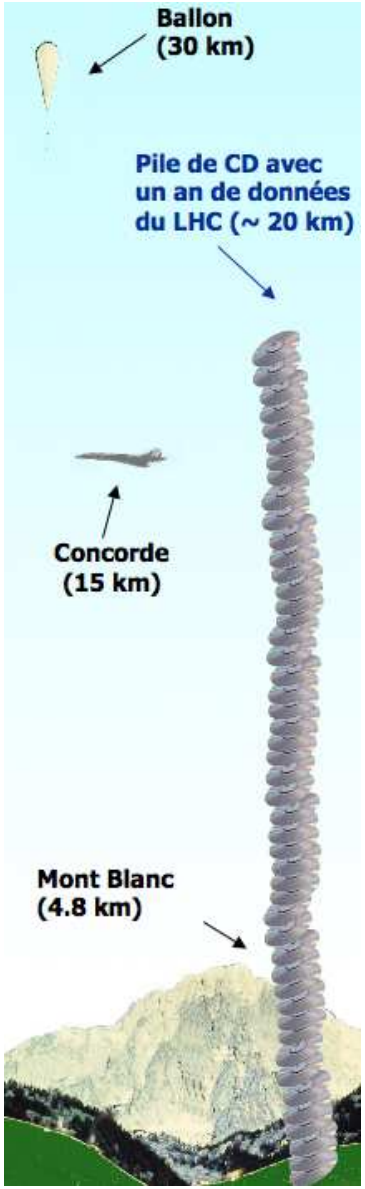

Largest SM matrices we treat contain $\sim 10^{14}$ non-zero matrix elements. They can not be stored on a hard drive. It would take 100.000 DVDs to store one matrix!

Shell gaps in nuclei & realistic 2-body interactions

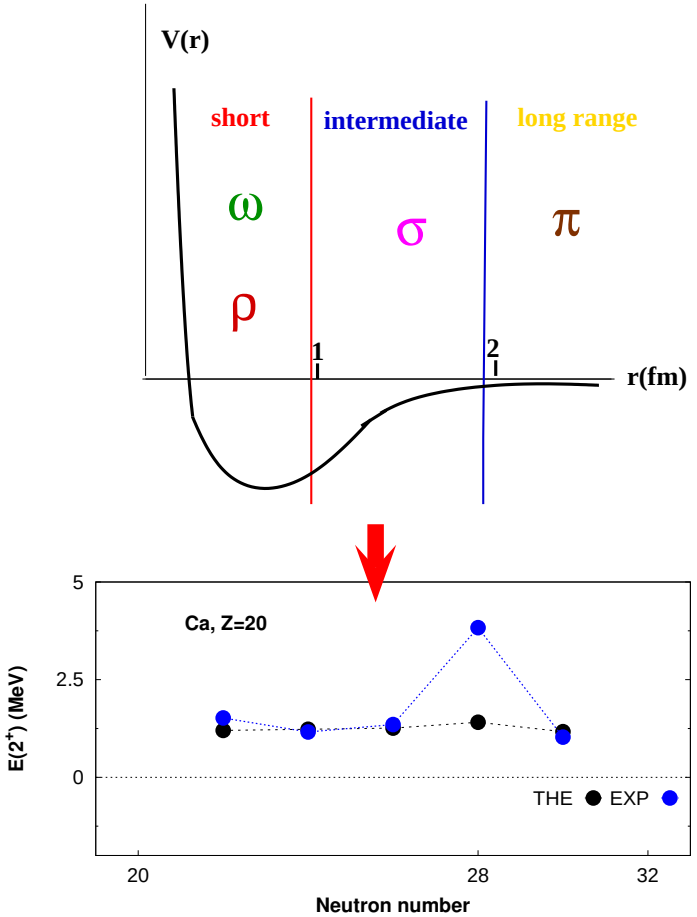

$$U(r) = \frac{1}{2}m\omega^2 r^2 + D\vec{l}^2 - C\vec{l}\cdot\vec{s}$$

- Realistic 2N potentials produce strong h.o. closures but no spin-orbit ones...

Shell Model & 3N forces

- No-core shell model calculations with 3N forces possible for light systems (A∼12).
- In core-shell model for heavier nuclei, 3N contribution taken into account empirically.

A. Cortes and A.P. Zuker, "Self-consistency and **many-body monopole forces** *in shell model calculations" Phys. Lett. B84* **(1979)** *25*

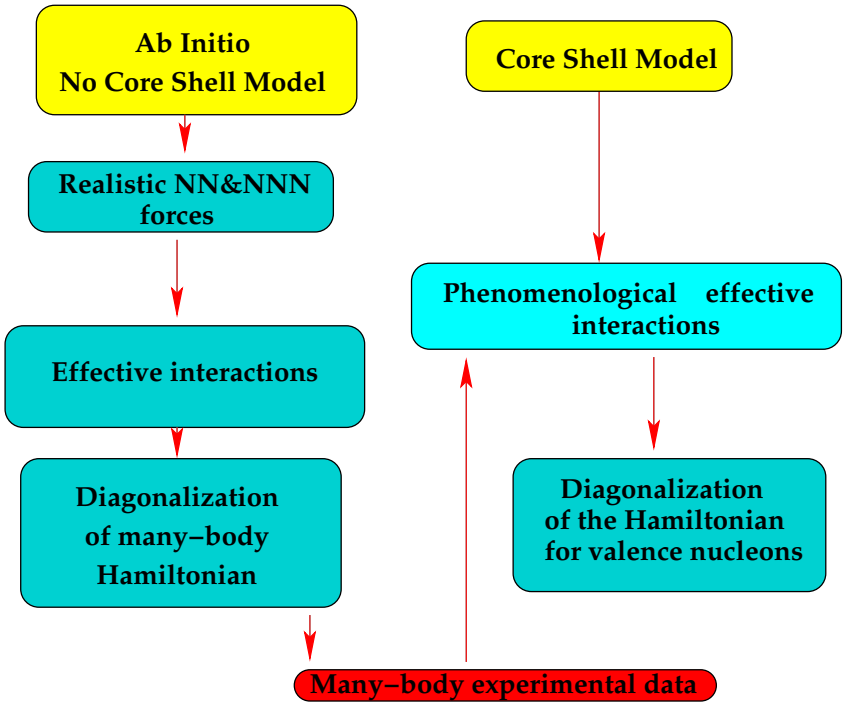

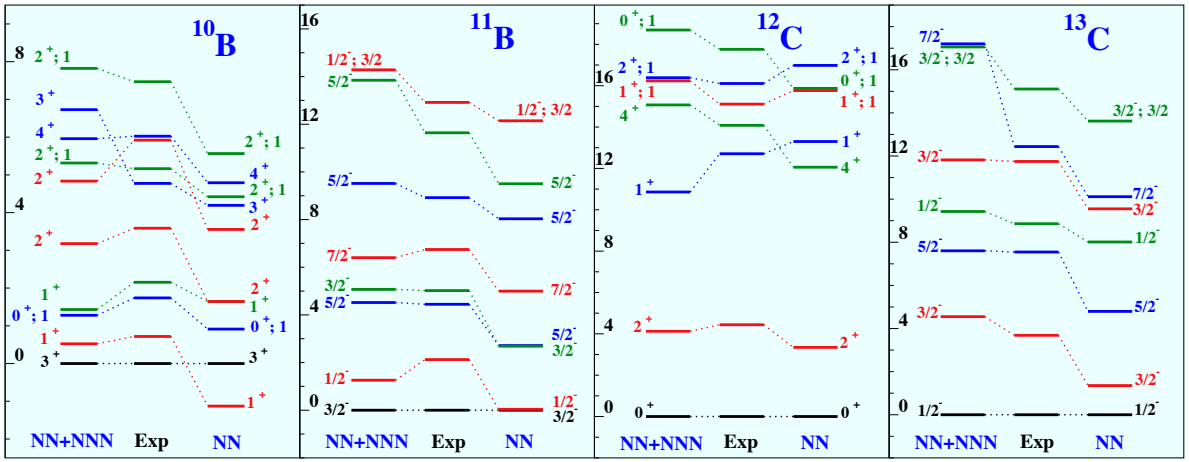

Excitation energies in light nuclei in NCSM with chiral EFT interactions. *P. Navratil et al., Phys. Rev. Lett. 99 (2007) 042501.*

SM with empirical interactions: regions of activity

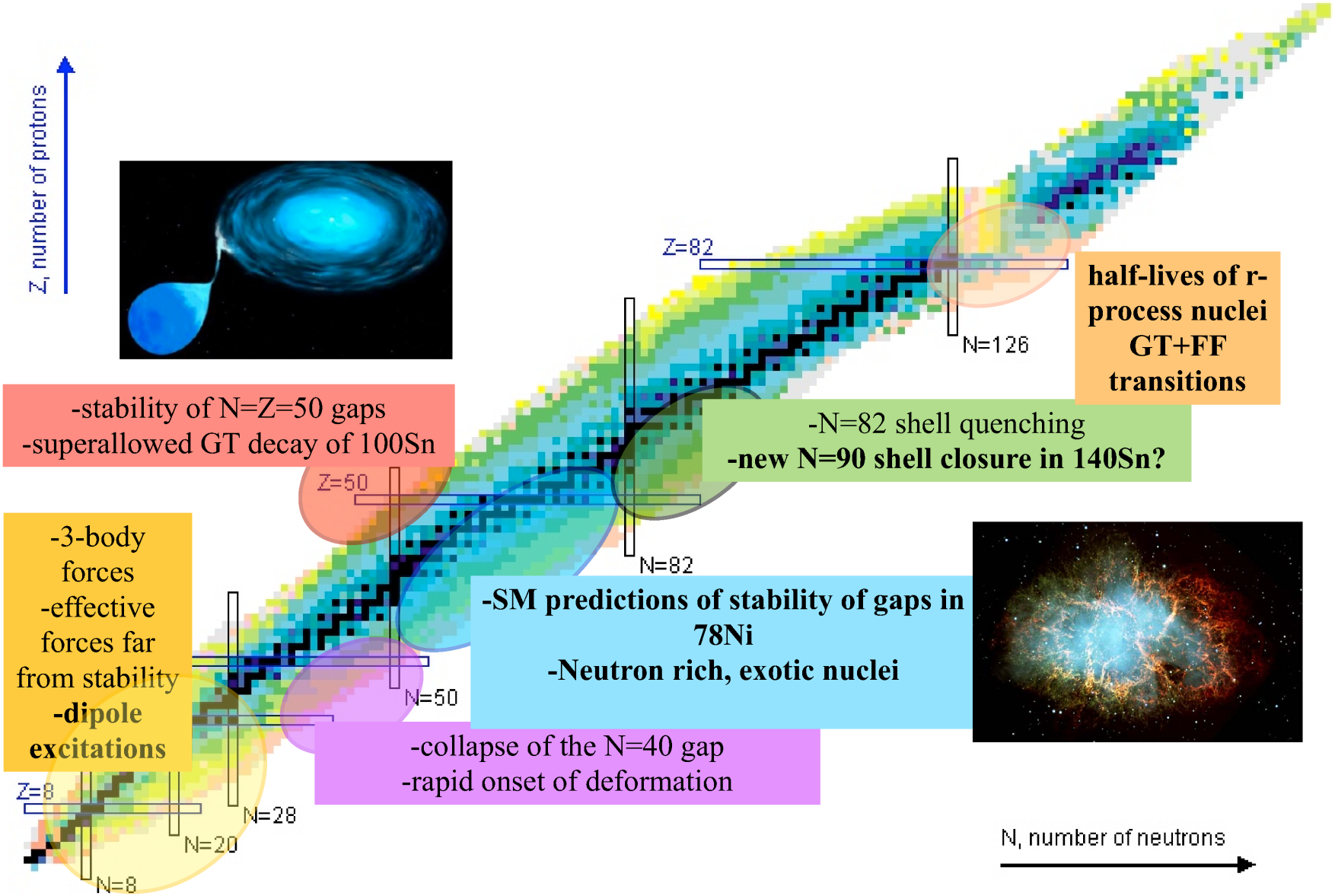

Shell evolution: what have we learned ?

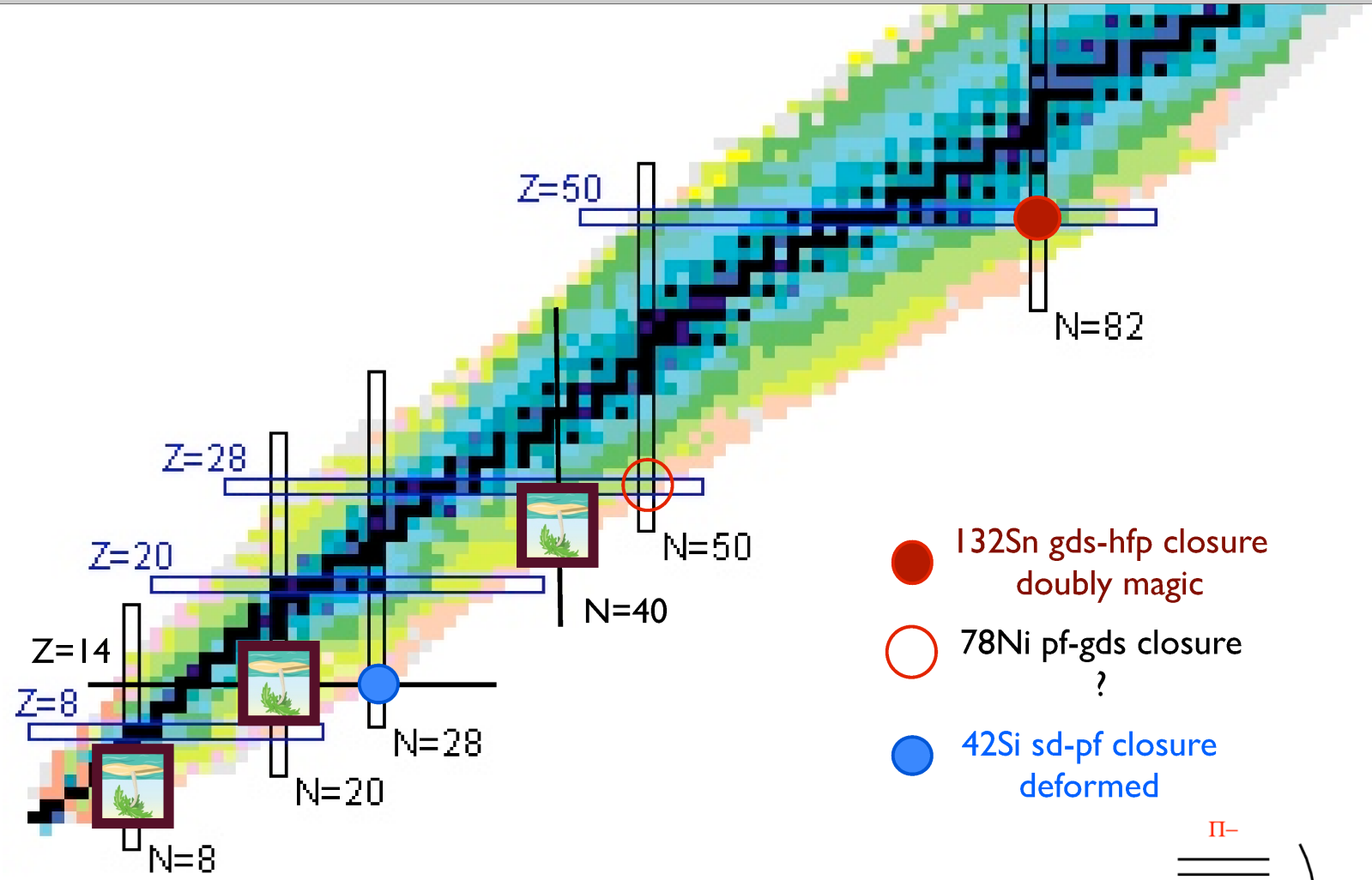

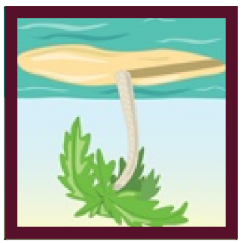

Island of inversion=region of sudden deformation in nuclei with a h.o. neutron shell closure

132Sn gds-hfp closure
doubly magic

78Ni pf-gds closure
?

42Si sd-pf closure
deformed

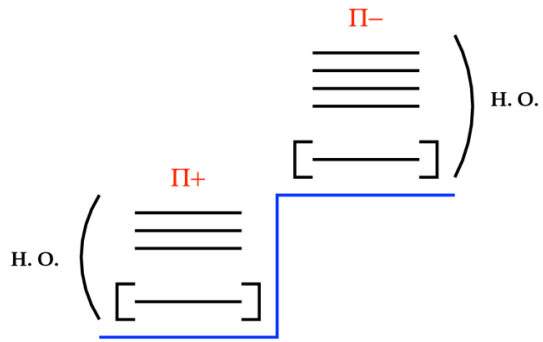

Stability of shell gaps in ^{78}Ni: the N=50 shell closure

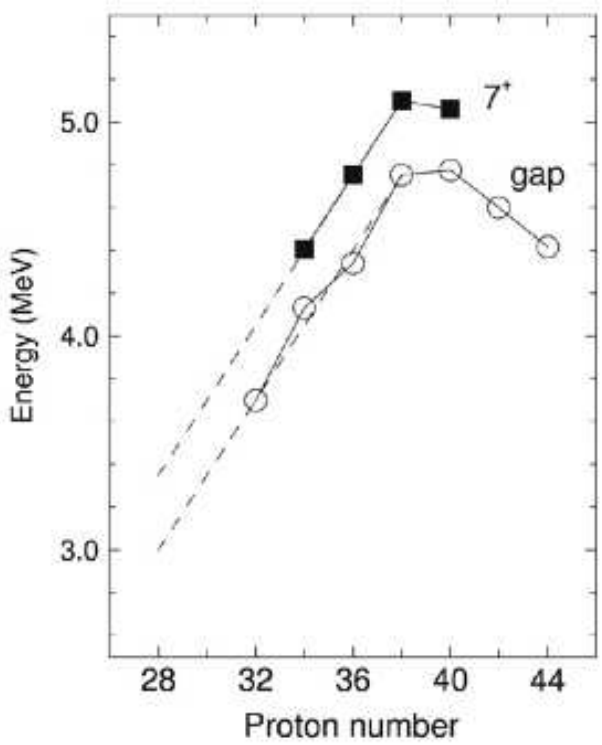

O.Sorlin, M.-G. Porquet,

Prog. Part. Nucl. Phys. 61 (2008) 602-673

- Experimental evidence at $Z = 32$ non conclusive
- Extrapolation of experimental data dangerous since shell efects are sudden
- Correlations in semi-magic nuclei hide the mean-field effects
- Theory essential for understanding of the shell evolution

Stability of shell gaps in ^{78}Ni: the N=50 shell closure

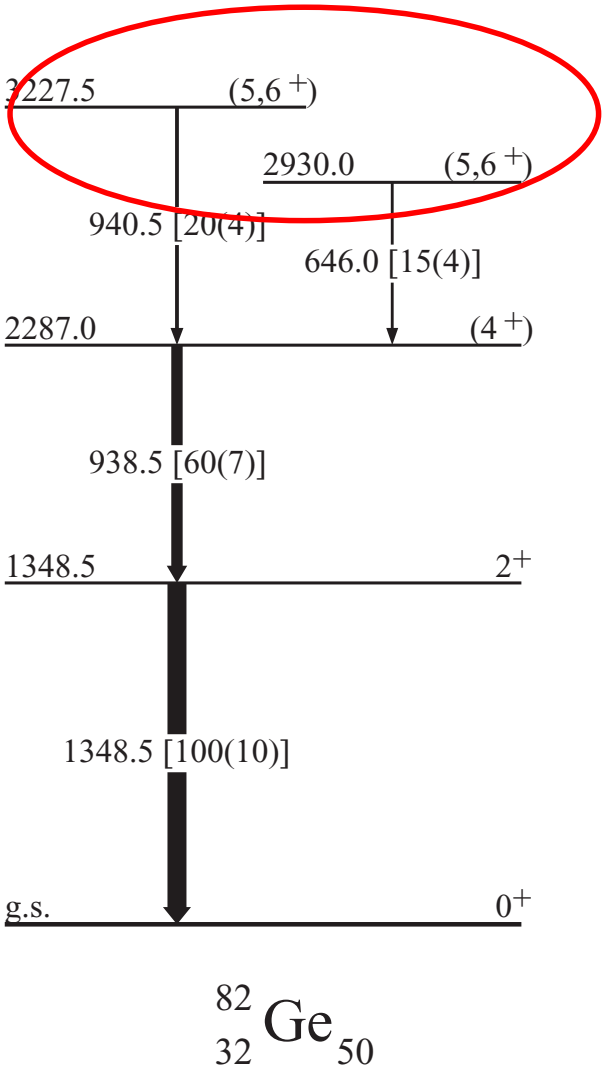

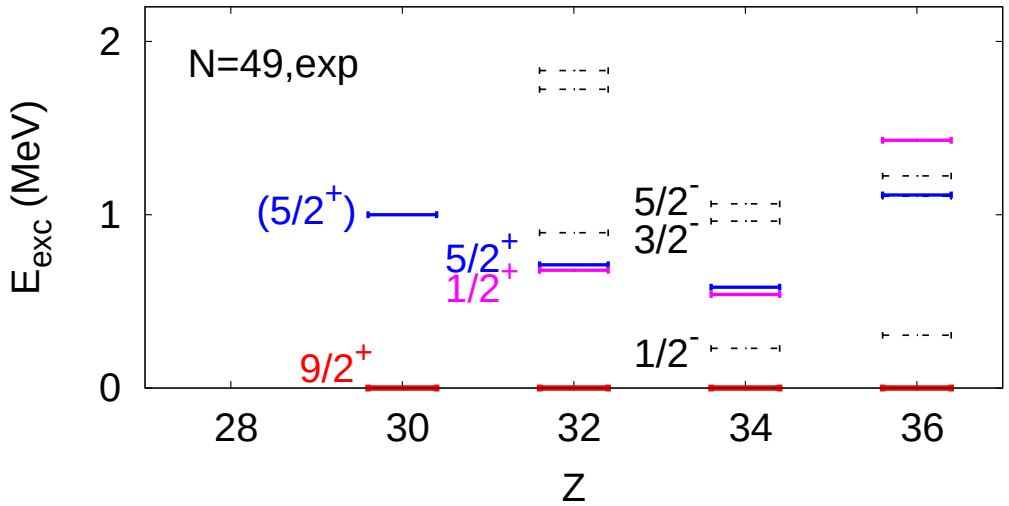

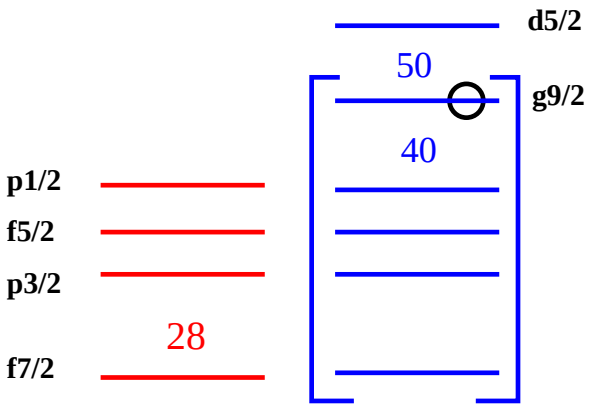

T. Rzaca-Urban et al., PRC 76 (2007) 027302

^{82}Ge and N=50 isotones

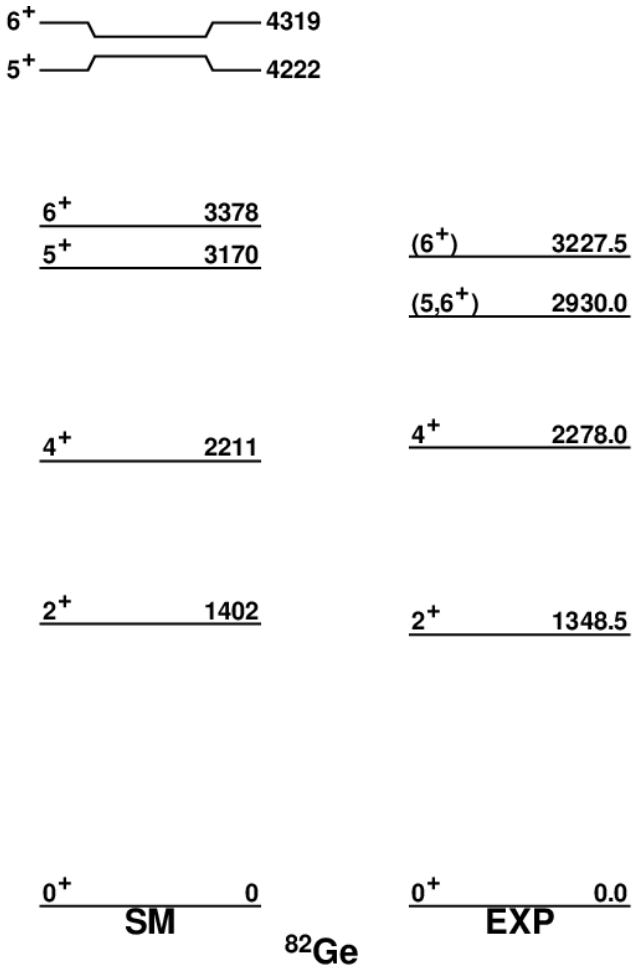

	protons			neutrons	
J^π	$f_{7/2}$	$f_{5/2}$	p	$g_{9/2}$	$d_{5/2}$
0^+	7.69	3.76	0.55	9.65	0.36
2^+	7.79	3.76	0.45	9.61	0.41
4^+	7.87	3.81	0.32	9.67	0.35
5^+	7.62	3.63	0.75	8.53	1.48
6^+	7.62	3.64	0.74	8.57	1.43

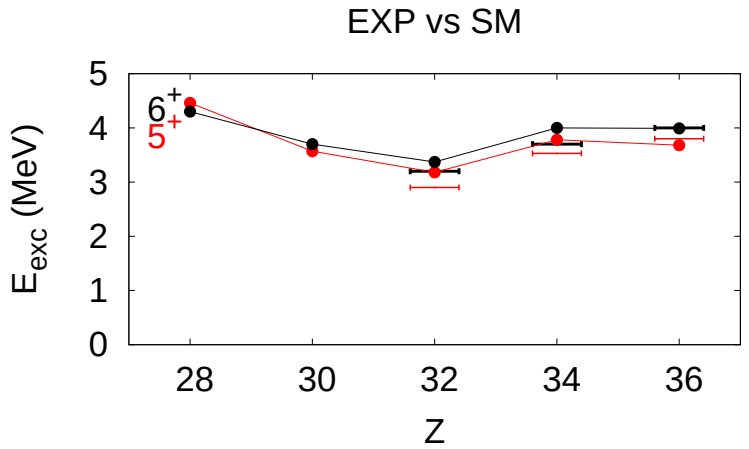

K. Sieja et al., Phys. Rev. C85 (2012) 051301R.

Levels across the N=50 gap: role of the correlations

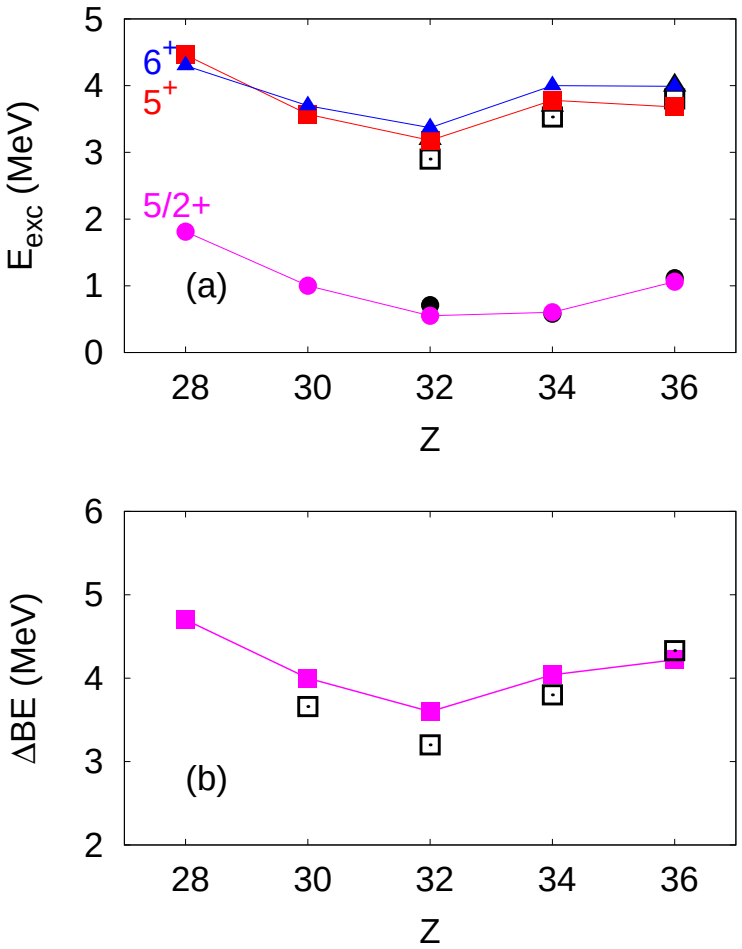

- Robustness of the N=50 gap in ^{78}Ni

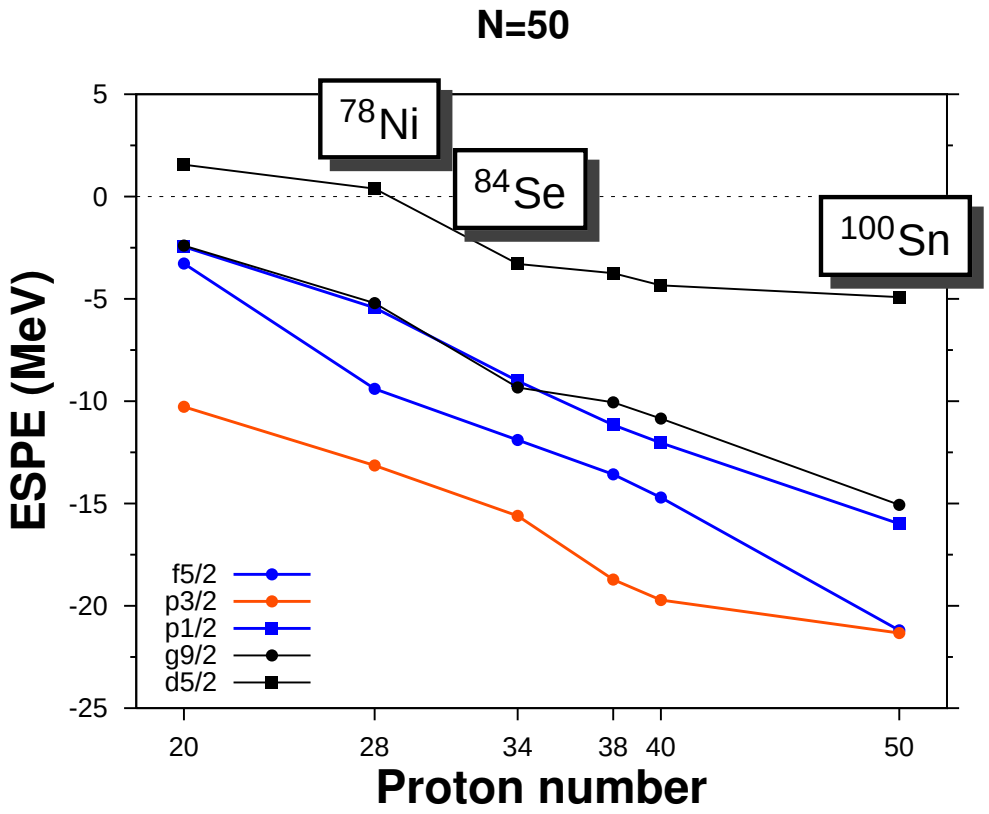

- No change of the $g_{9/2}$-$d_{5/2}$ splitting between Ni and Se
- Possibility of evaluating (n,γ) cross sections around $A = 80$

Shell evolution along isotopic chains and 3N forces

K. Sieja et al., Phys.Rev.C85 (2012) 051301(R)

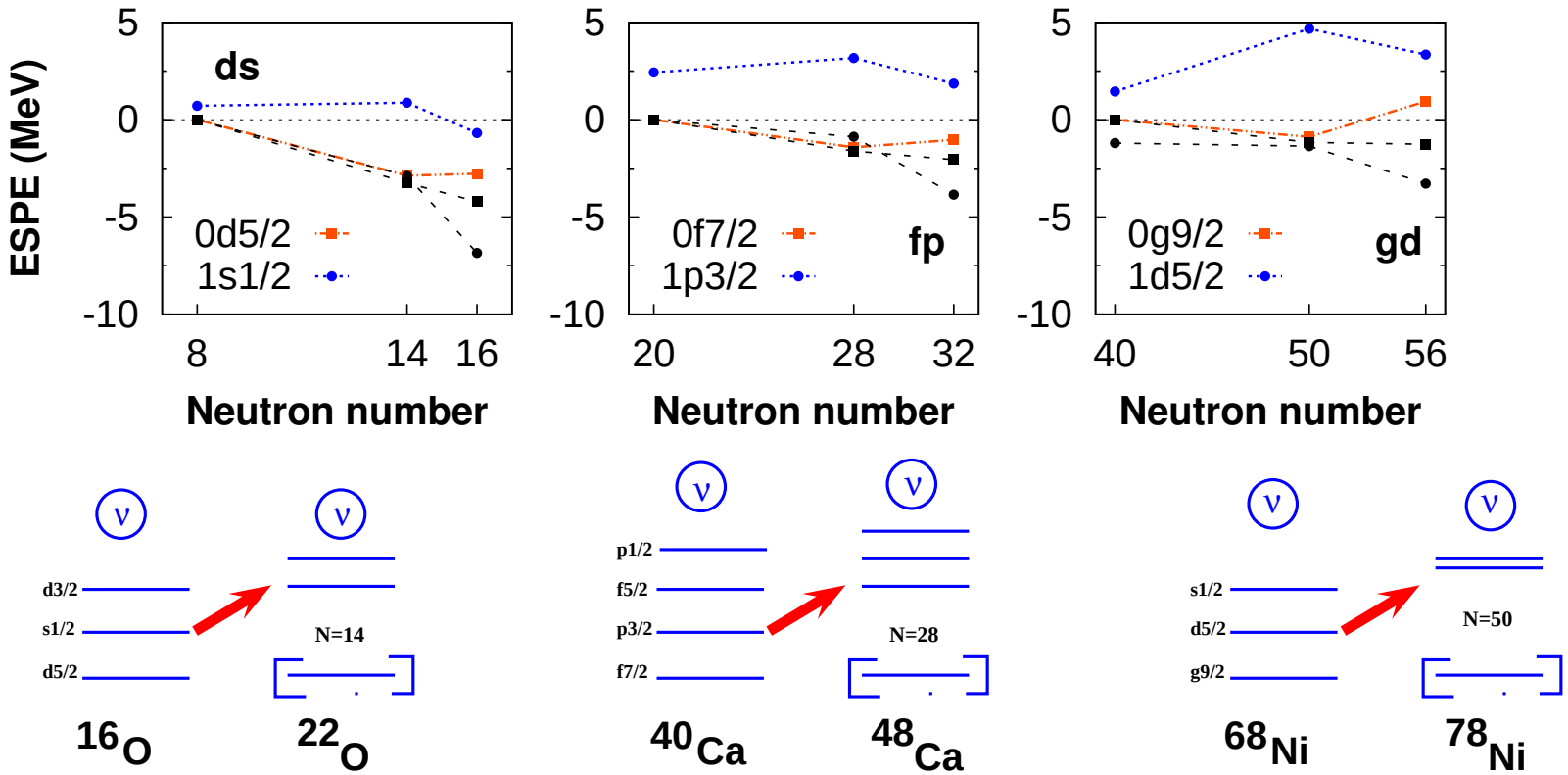

☞Shell model predictions for the $N = 50$ gap consistent with 3N effects observed in light nuclei!

A. P. Zuker, Phys. Rev. Lett. 90 (2003) 042502

☞Understanding three-body mechanisms essential for modeling of shell evolution in nuclear physics. Ideas how to improve DZ mass formula based on what we know about the role of 3N forces in the creation of shell gaps *J. Mendoza-Temis et al., Nuc. Phys. A843 (2010) 14-36*.

3N forces: a new shell closure at N=90?

PHYSICAL REVIEW C **81**, 064328 (2010)

New shell closure for neutron-rich Sn isotopes

S. Sarkar*
Department of Physics, Bengal Engineering and Science University, Shibpur, Howrah 711103, India

M. Saha Sarkar†
Nuclear Physics Division, Saha Institute of Nuclear Physics, Kolkata 700064, India

(Received 11 October 2009; revised manuscript received 11 June 2010; published 29 June 2010)

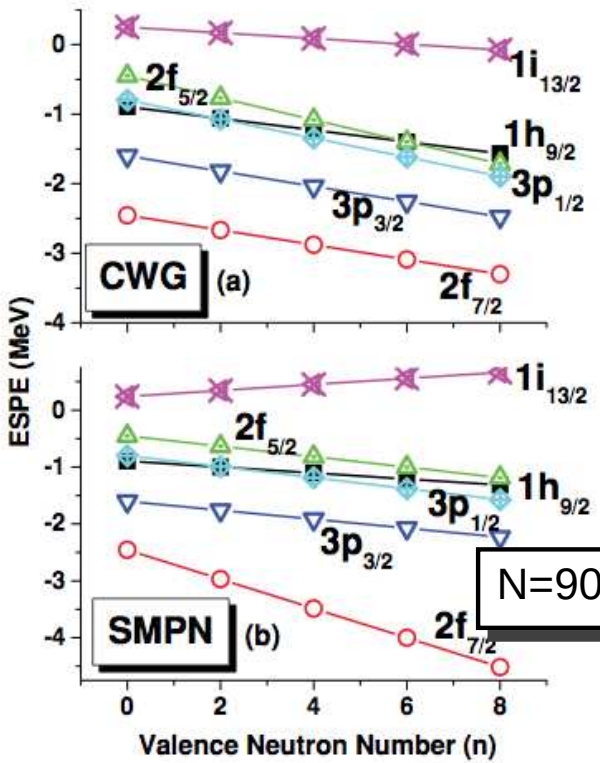

N=90 gap =2.5MeV

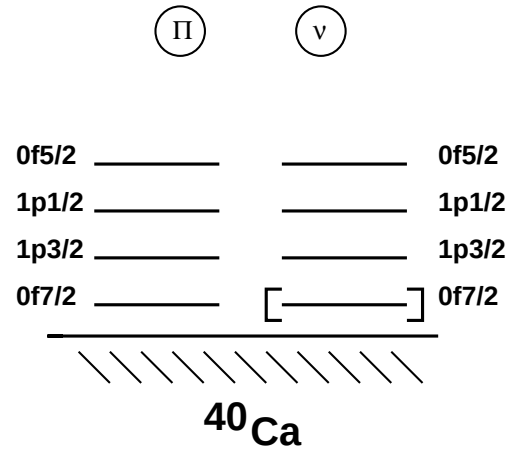

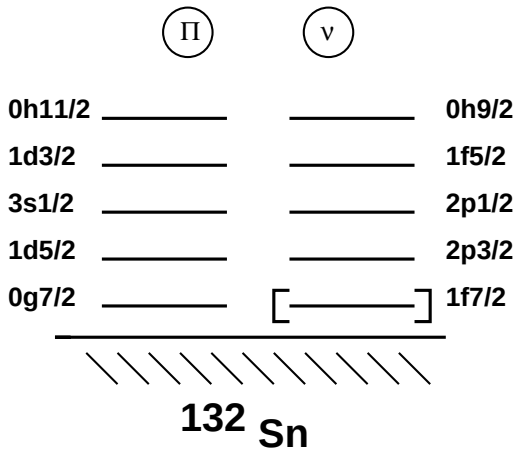

Can one make analogy between ^{48}Ca and ^{140}Sn?

Role of nuclei around N=90

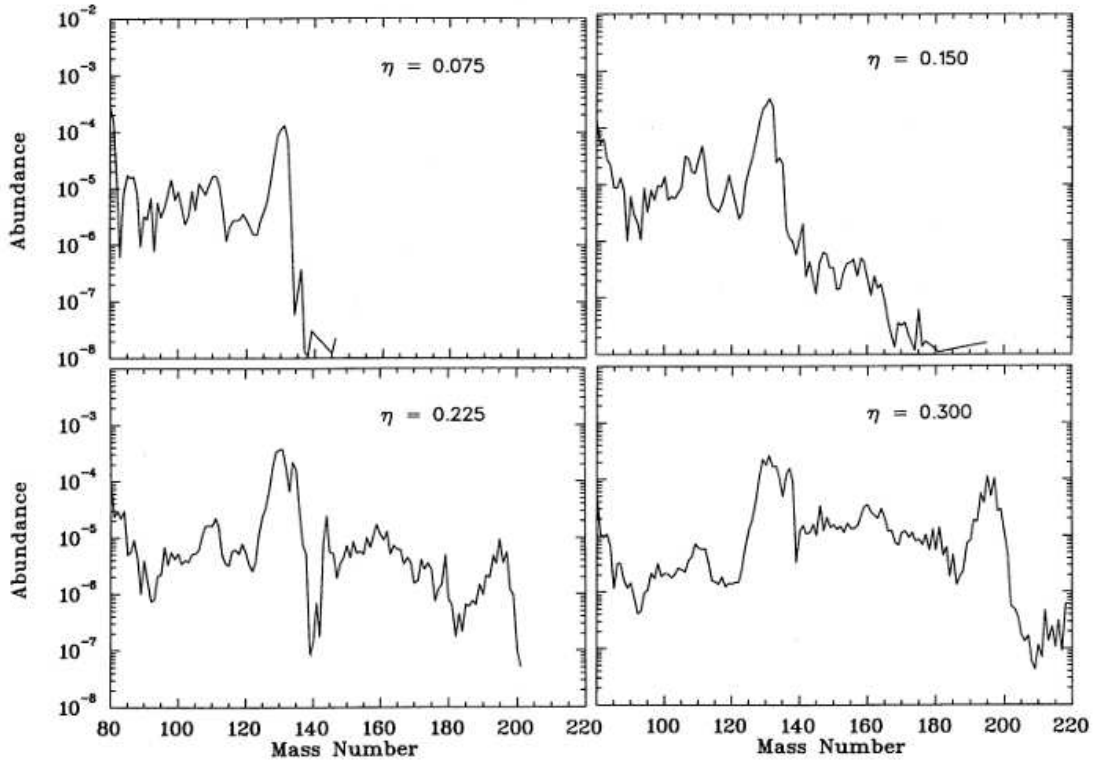

FIG. 4.—Comparison of final calculated *r*-process abundances for material with initial neutron excesses of (*a*) $\eta = 0.075$; (*b*) $\eta = 0.15$; (*c*) $\eta = 0.225$; and (*d*) $\eta = 0.3$. Note that low η and hence low neutrons per seed are needed to contribute to the $A = 130$ peak, whereas the $A = 195$ peak is produced at higher values for η.

stand the solar-system abundance pattern. The need for a distribution of neutron exposures in the *r*-process has been appreciated for some time (e.g., Seeger et al. 1965; Kodama & Takahashi 1975; Hillebrandt et al. 1976) and has recently been more quantitatively established in the work of Kratz et al. (1992). In the present work we identify how such a superposition might naturally arise from the ejection of regions of differing η and/or ϕ from the expanding hot bubble. As mentioned above, the superposition giving rise to the solar-system *r*-process abundance distribution is probably a curve in the parameter space of η, ϕ, and expansion time scale rather than

therefore cannot be due to the *r*-process itself. It must, therefore, arise from an effect which occurs after the neutrons freeze out. We have discovered that most of this dip can be attributed to photodisintegration of a single nucleus, ^{139}Te. The photodisintegretion rate for this nucleus is higher than that of neighboring nuclei because it has a smaller binding energy ($\sim$1.5 MeV) than neighboring nuclei ($\sim$2.5 MeV). The reason for such a small neutron binding energy for this nucleus in the Möller (1991) mass formula is that it falls on the edge of a transition region from spherical to deformed nuclei. Although

B.S. Meyer et al., Astr. Journal 399 (1992) 656

Structure at N=90 and r-process

- Masses around $N = 90$ determine the mass flow from the second to third r-process peaks (NS mergers)

Calculations from PhD thesis of J. Mendoza-Temis

(TU Darmstadt)

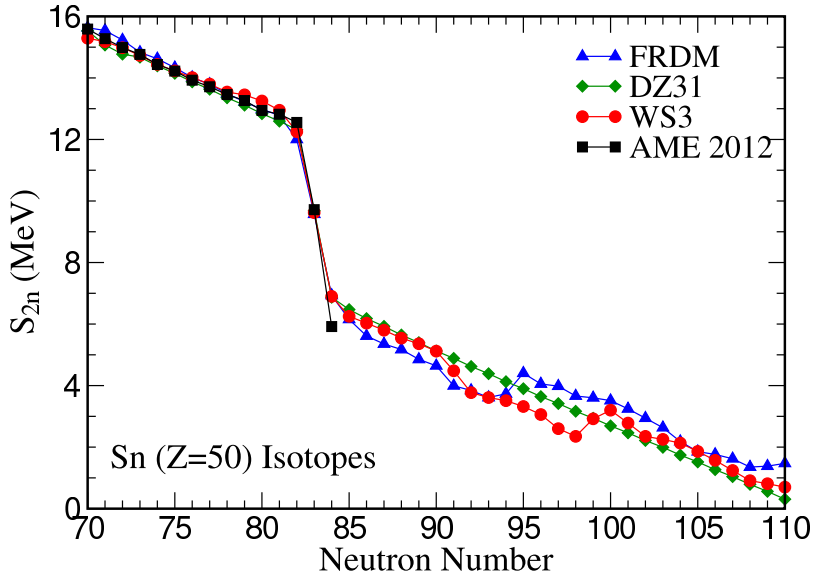

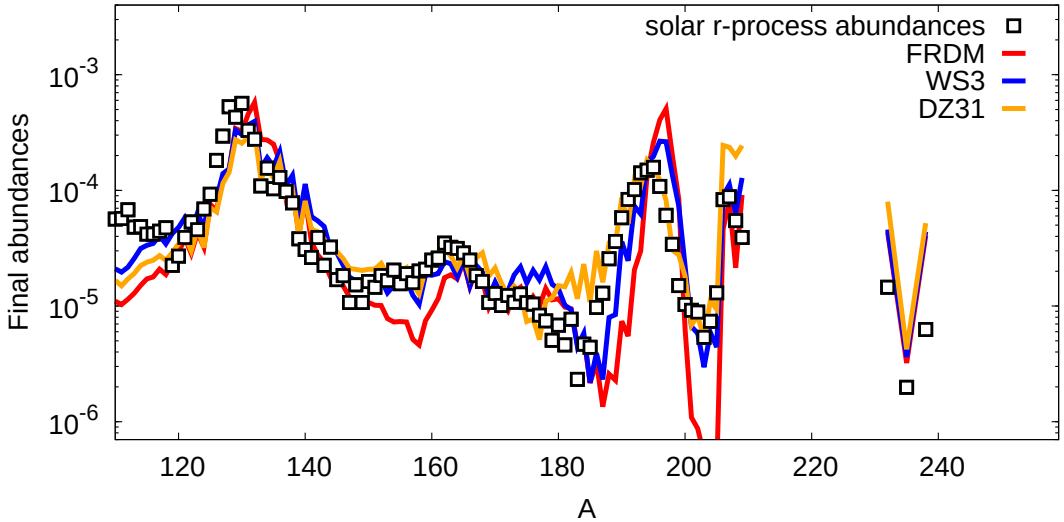

Seniority isomers in the tin chain

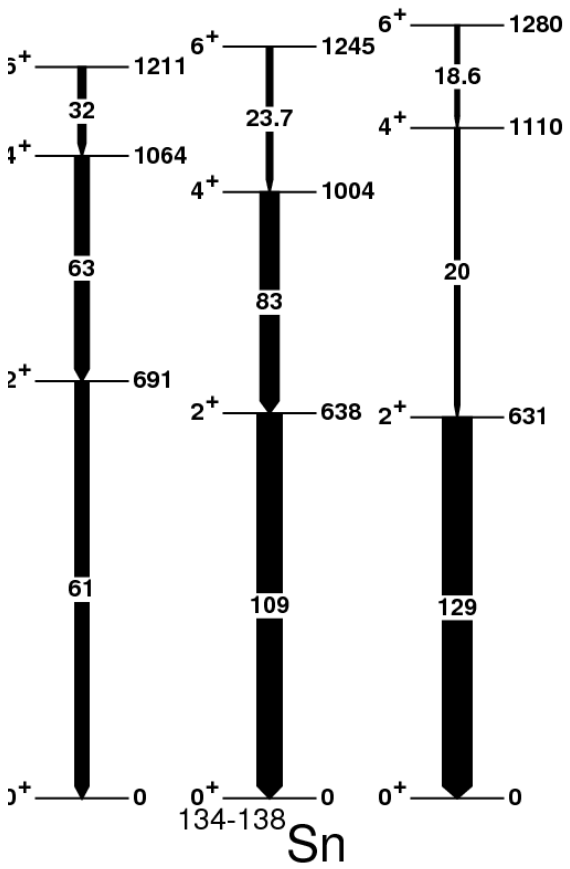

Exp - PhD work of G. Gey (LPSC Grenoble)

G. Simpson, G. Gey et al., submitted to PRL

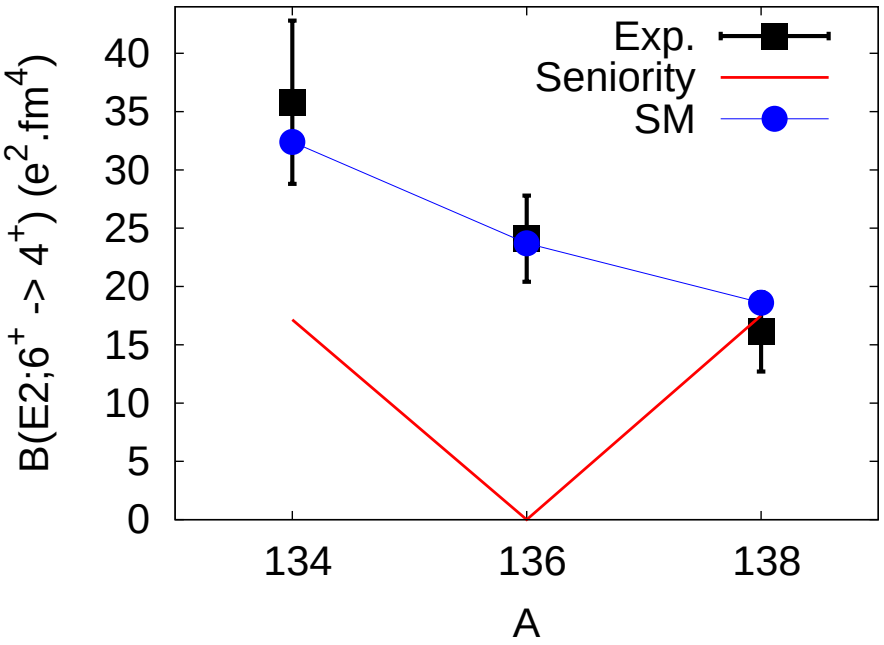

- Previous SM calculations wrong by a factor 2 for the $B(E2;6^+ \rightarrow 4^+)$ in ^{136}Sn
- Important seniority mixing effects in ^{136}Sn
- Data compatible with a $f_{7/2} - p_{3/2}$ gap $<$1.5 MeV in present SM calculations

$$B(E2; vJ \rightarrow vJ-2) \sim \left(1 - \frac{2n}{(2j+1)}\right)^2$$

☞Study of masses in this region in the present SM framework in progress

Neutron capture cross sections

$$\sigma^{\mu\nu}_{(n,\gamma)}(E_i,n) = \frac{\pi\hbar^2}{2M_{i,n}E_{i,n}} \frac{1}{(2J_i^{\mu}+1)(2J_n+1)} \sum_{J,\pi}(2J+1)\frac{T_n^{\mu}T_{\gamma}^{\nu}}{T_{tot}},$$

where:
$E_{i,n}, M_{i,n}$- center-of-mass energy, reduced mass of the system
$J_n = 1/2$-neutron spin
transmission coefficients:
$T_n^{\mu} = T_n(E,J,\pi;E_i^{\mu},J_i^{\mu},\pi_i^{\mu})$ $T_{\gamma}^{\nu} = T_{\gamma}(E,J,\pi;E_m^{\nu},J_m^{\nu},\pi_m^{\nu})$

For a given multipolarity

$$T_{XL}(E,J,\pi,E^{\nu},J^{\nu},\pi^{\nu}) = 2\gamma^{2L+1} f_{XL}(E,E_{\gamma})$$

Key ingredients in Hauser-Feschbach calculations:

- description of gamma emission spectra of a compound nucleus
- Brink-Axel hypothesis

Lanczos strength function method

$$S = |\hat{O}|\psi_i\rangle| = \sqrt{\langle\psi_i|\hat{O}^2|\psi_i\rangle}$$

The operator $\hat{O}$ does not commute with H and $\hat{O}|\psi_i\rangle$ is not necessarily the eigenstate of the Hamiltonian. But it can be developed in the basis of energy eigenstates:

$$\hat{O}|\psi_i\rangle = \sum_f S(E_f)|E_f\rangle,$$

where $S(E_f) = \langle E_f|\hat{O}|\psi_i\rangle$ is called **strength function**.

If we carry Lanczos procedure using $|O\rangle = \hat{O}|\psi_i\rangle$ as initial vector then H is diagonalized to obtain eigenvalues $|E_f\rangle$ and after N iterations we have the also the strength function:
$\tilde{S}(E_f) = \langle E_f|O\rangle = \langle E_f|\hat{O}|\psi_i\rangle$.

How good is the strength function $\tilde{S}$ after N iterations compared to the exact one S?

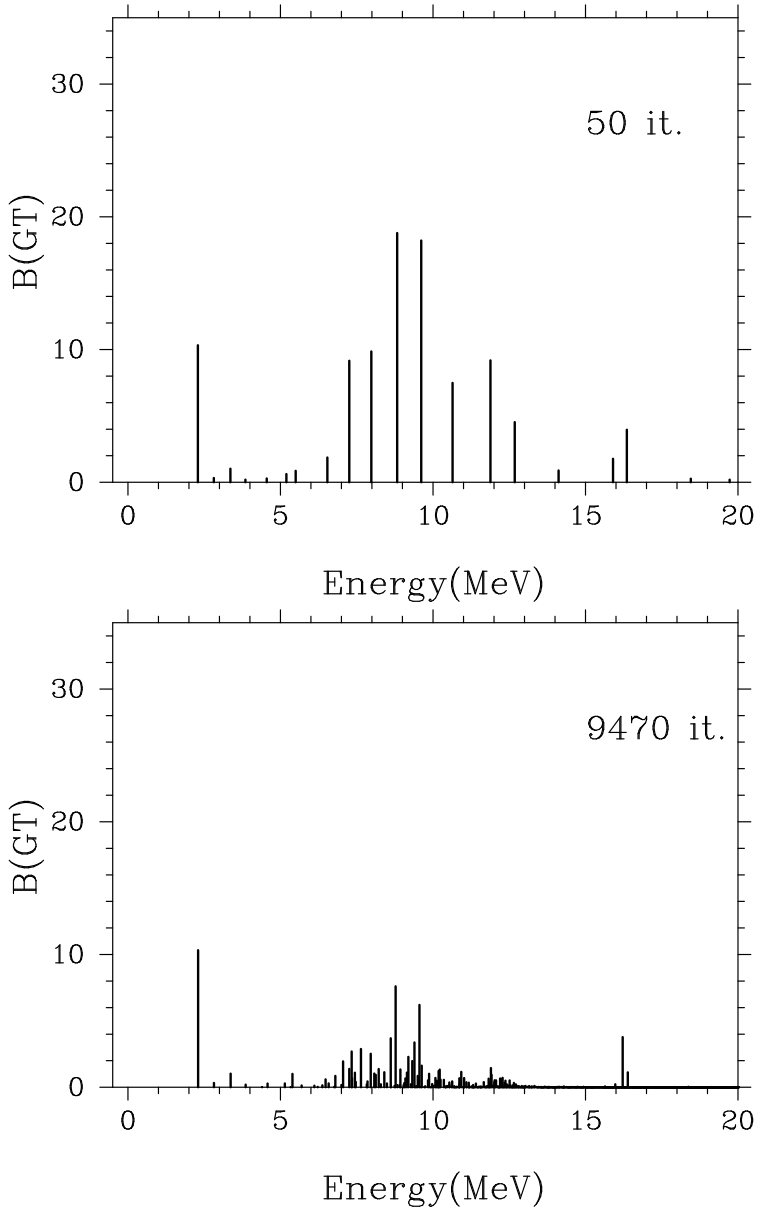

Lanczos strength function method

$$S = |\hat{O}|\psi_i\rangle| = \sqrt{\langle\psi_i|\hat{O}^2|\psi_i\rangle}$$

The operator $\hat{O}$ does not commute with H and $\hat{O}|\psi_i\rangle$ is not necessarily the eigenstate of the Hamiltonian. But it can be developed in the basis of energy eigenstates:

$$\hat{O}|\psi_i\rangle = \sum_f S(E_f)|E_f\rangle,$$

where $S(E_f) = \langle E_f|\hat{O}|\psi_i\rangle$ is called **strength function**.

If we carry Lanczos procedure using $|O\rangle = \hat{O}|\psi_i\rangle$ as initial vector then H is diagonalized to obtain eigenvalues $|E_f\rangle$ and after N iterations we have the also the strength function:
$\tilde{S}(E_f) = \langle E_f|O\rangle = \langle E_f|\hat{O}|\psi_i\rangle$.

How good is the strength function $\tilde{S}$ after N iterations compared to the exact one S?

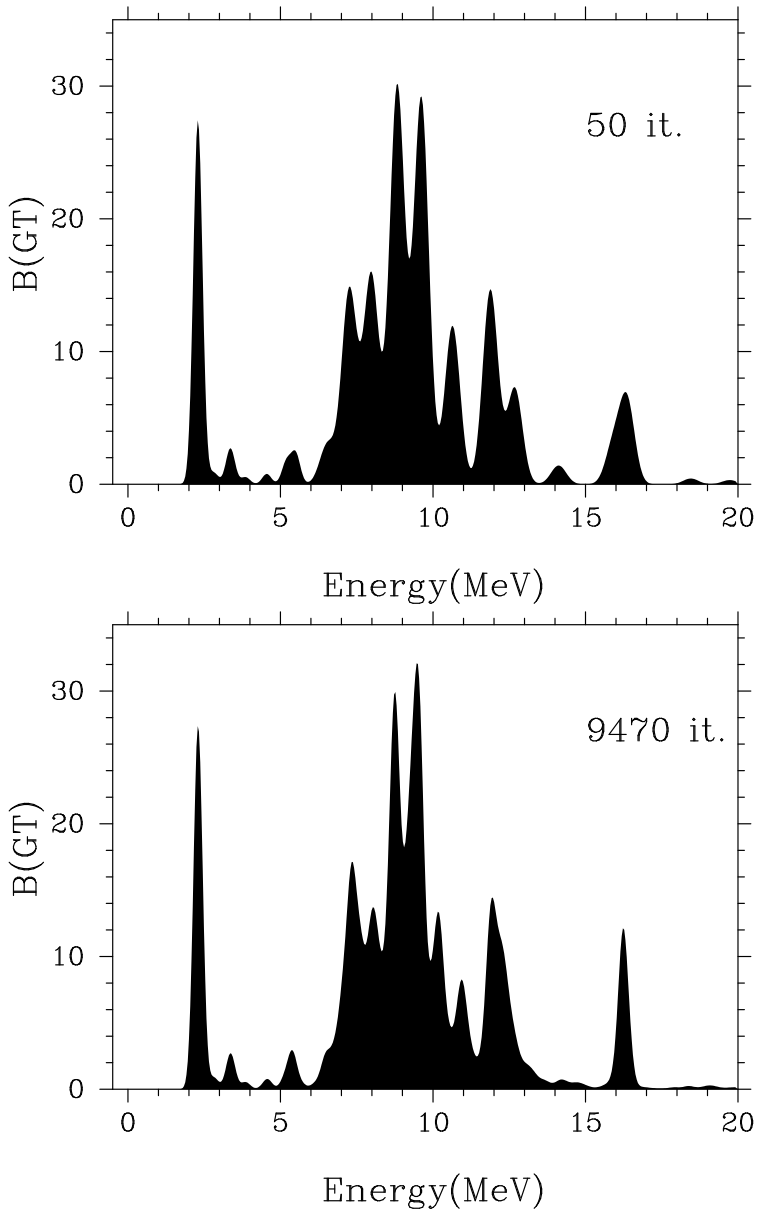

Impact of the realistic M1 fragmentation on the neutron capture cross sections

M1 microscopic strength functions in iron chain (^{53}Fe-^{70}Fe), impact on (n,γ) cross sections, tests of Brink-Axel hypothesis

H.-P. Loens K. Langanke, G. Martinez-Pinedo and K. Sieja, EPJ A48 (2012) 48

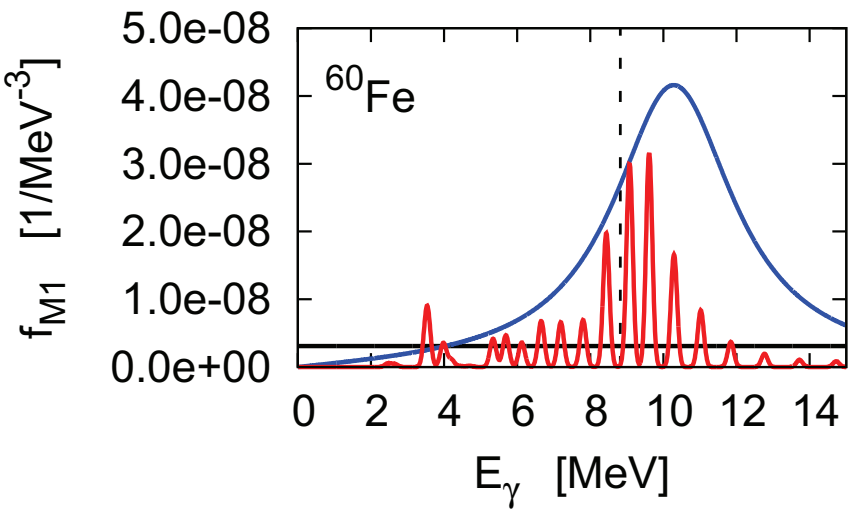

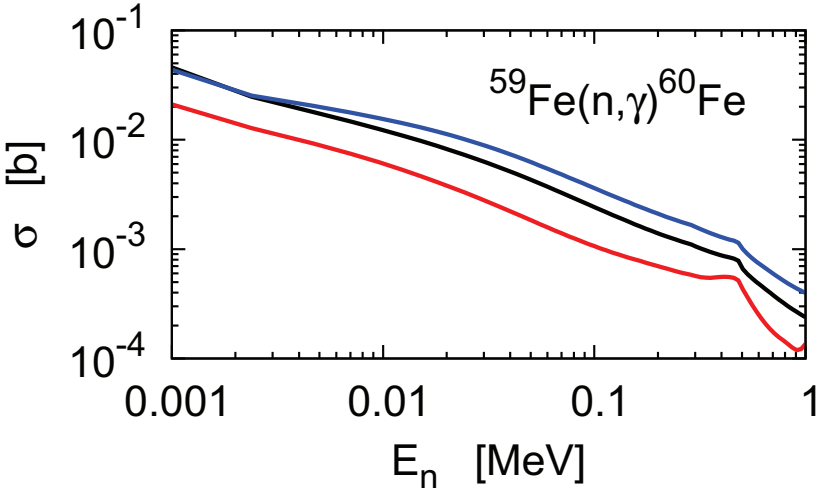

- State-by-state cross section 2 times larger than using Brink hypothesis
- Using SF of 2^+ state instead of 0^+ leads to larger cross sections

Impact of the realistic M1 fragmentation on the neutron capture cross sections

H.-P. Loens K. Langanke, G. Martinez-Pinedo and K. Sieja, EPJ A48 (2012) 48

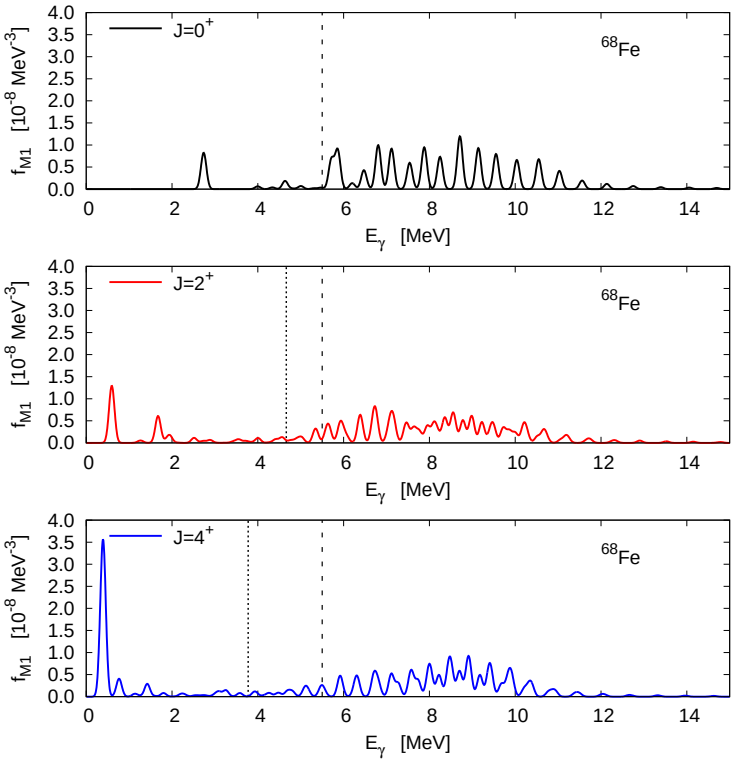

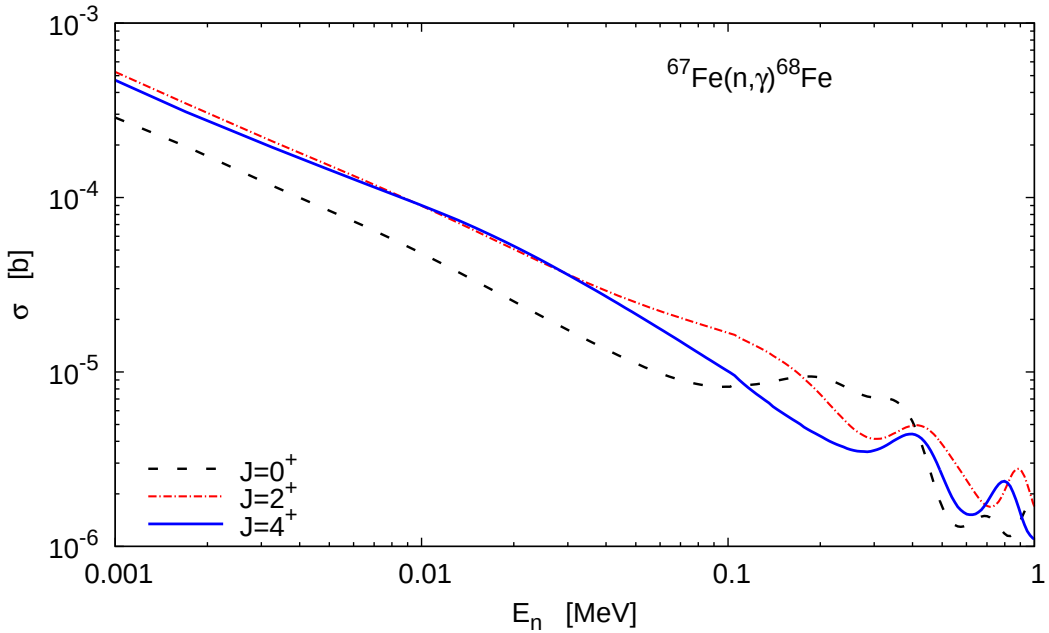

- State-by-state cross section 2 times larger than using Brink hypothesis
- Using SF of 2^+ state instead of 0^+ leads to larger cross sections

Low energy enhancement of the γ-strength function

Data from Oslo group

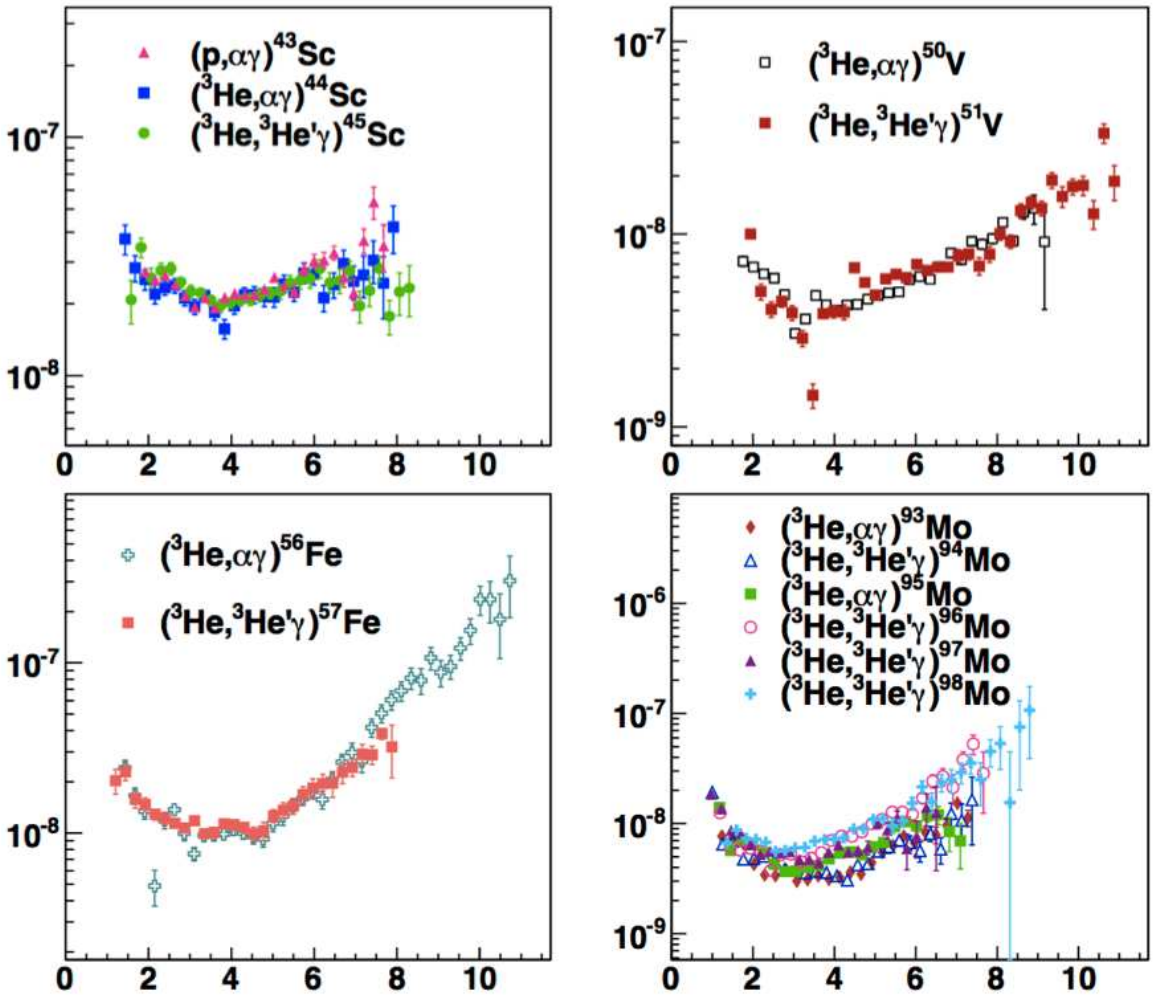

- Microscopic strength functions are different from global parametrizations
- Low energy enhancement of γ-strength observed in different regions of nuclei
- It can influence the (n,γ) rates of the r-process by a factor of 10!

  A.C. Larsen and S. Goriely, Phys. Rev. C82 (2010) 014318
- Evidence for the dipole nature of low energy enhancement in ^{56}Fe

  A. C. Larsen et al., Phys. Rev. Lett. 111 (2013) 242504

What theory says about it?

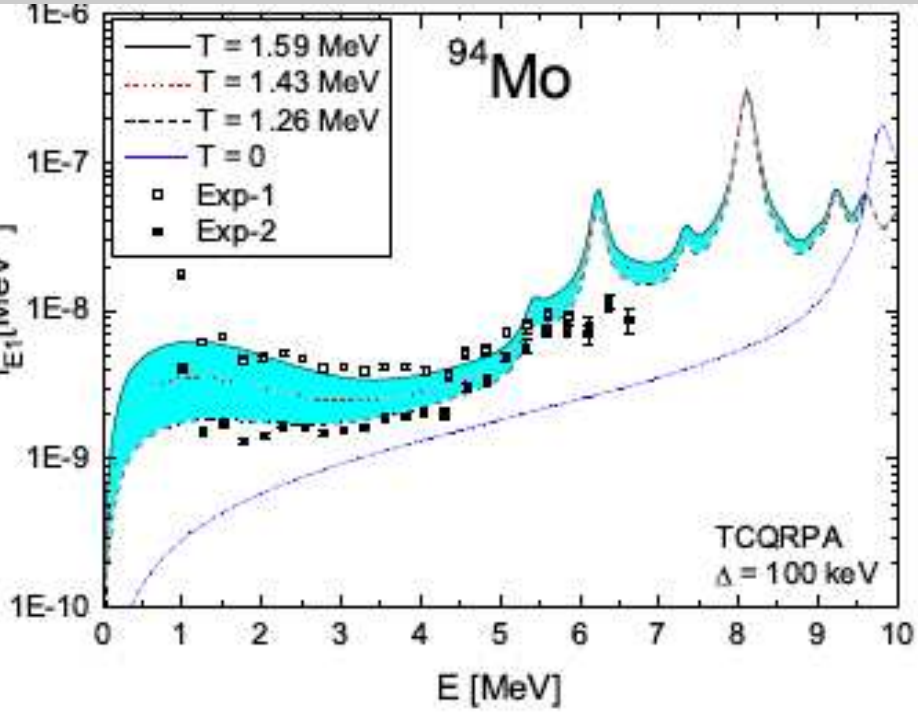

E. Litvinova and N. Belov, Phys. Rev. C88 (2013) 031302R

- Thermal continuum QRPA calculations
- Enhancement due to transitions between thermally unblocked s.p. states and the continuum
- Note the difference between $T = 0$ (ground state) and $T > 0$ (excited state) E1 strength distribution

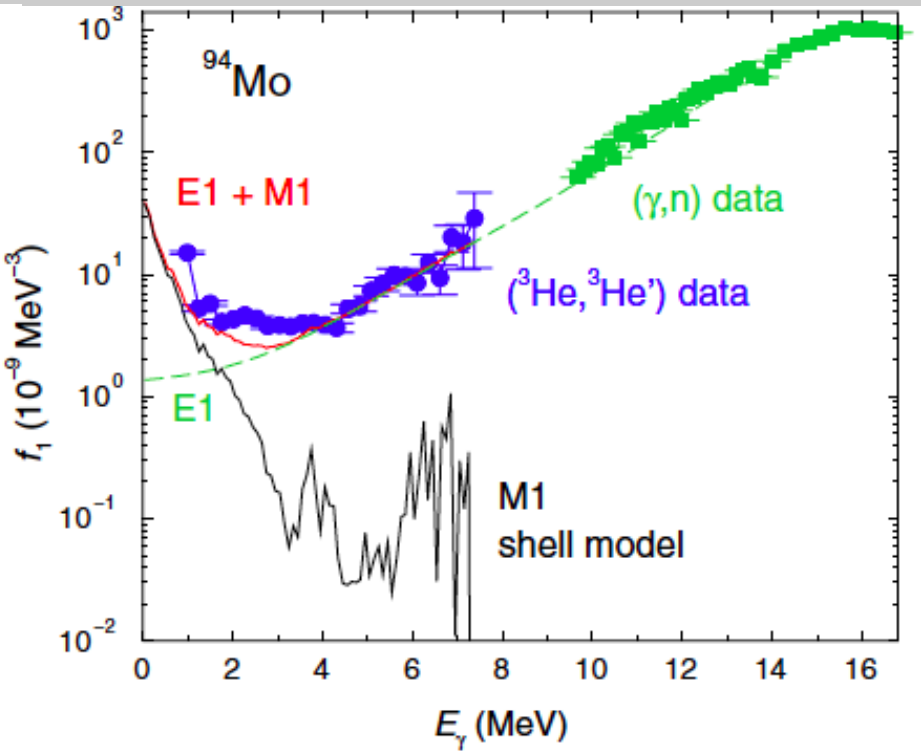

R. Schwengner et al., Phys. Rev. Lett. C88 (2013)

- Shell model transitions between a large amount of states (more than 14000 transitions for each parity)
- Enhancement due to the transitions between states in the region near the quasicontinuum
- A general mechanism that can be found in other mass regions

M1-strength SM calculations in ^{94}Mo

R. Schwengner et al., Phys. Rev. Lett. C88 (2013)

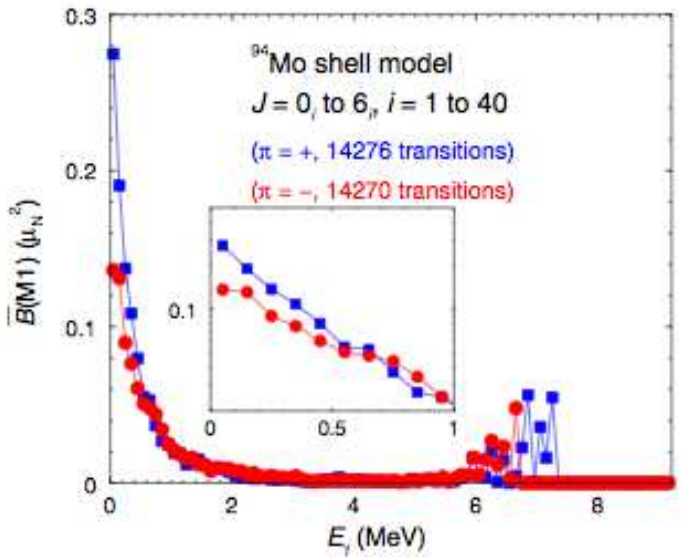

KS, present SM

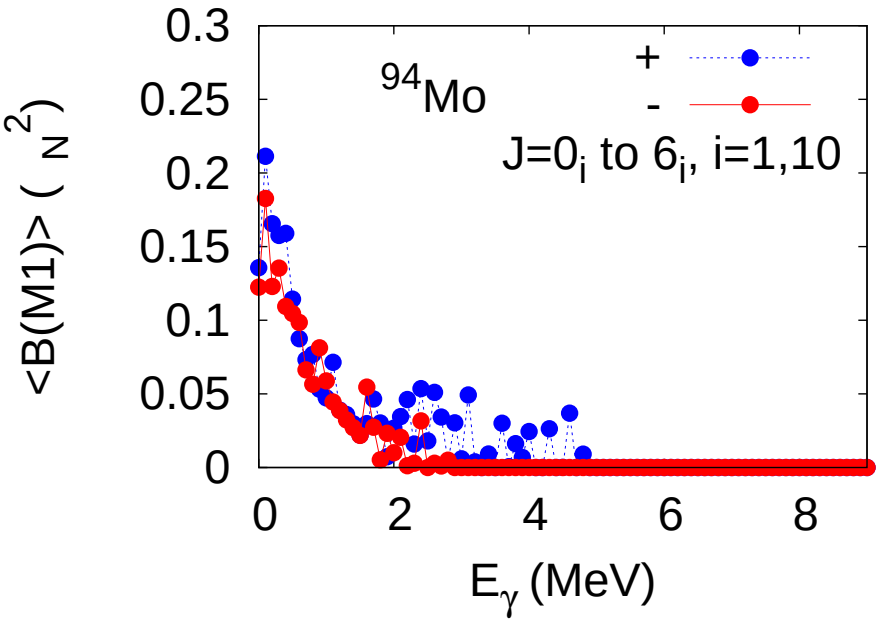

Model space:
$\pi(0f_{5/2}, 1p_{3/2}, 1p_{1/2}, 0g_{9/2})$
$\nu(0g_{9/2}, 1d_{5/2}, 0g_{7/2})$

Model space:
$\pi(0f_{5/2}, 1p_{3/2}, 1p_{1/2}, 0g_{9/2})$
$\nu(1d_{5/2}, 0g_{7/2}, 1d_{3/2}, 2s_{1/2}, 0h_{11/2})$

☞Low energy M1 enhancement independent on details of calculations: model space, interaction & number of states

M1-strength SM calculations in sd-pf shell nuclei

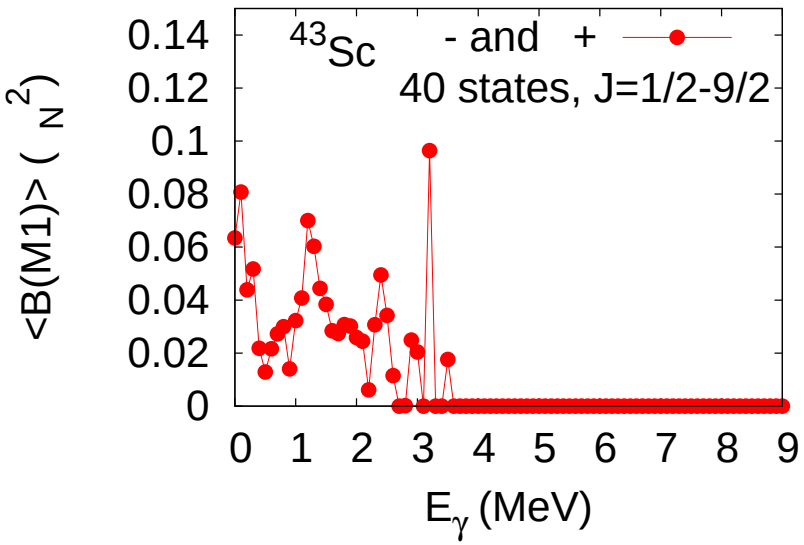

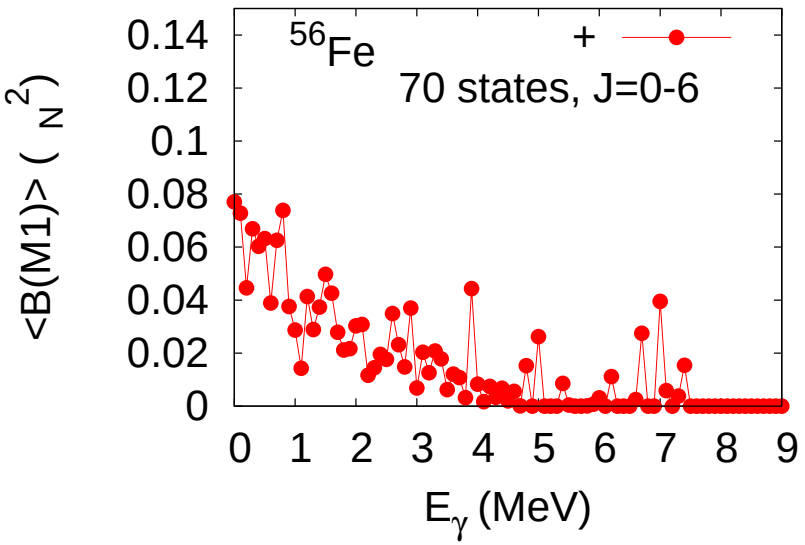

Open questions:

- Mechanism of enhancement ? The same in all nuclei?
- EM character, multipolarity.
- Which nuclei?

☞Further theoretical effort necessary to describe consistently E1/M1/E2 transitions in different regions

Summary

- Thanks to the progress in computing more and more regions of nuclei are accessible to SM diagonalizations, which provide currently the most accurate description of nuclear properties.
- Understanding of the mechanisms driving shell evolution (3N forces, tensor forces) allows for a better modelling all over the nuclear chart.
- Consistent description of gamma-excitation M1/E1/E2 strength functions is possible in the SM, for the moment in sd nuclei, soon also in the sd-pf region.

Thanks to:
E. Caurier, H. Naidja, F. Nowacki (IPHC Strasbourg)
G. Martinez-Pinedo, J. Mendoza-Temis (TU Darmstadt)

Modern theory of nuclear forces

- QCD is a gauge field theory which describes the strong interactions of color quarks and gluons (one universal coupling constant).
- There are six quarks $q = (u, d, s, c, b, t)$ and 8 gluons.
- The QCD Lagrangian can be written

$$\mathscr{L}_{QCD} = \mathscr{L}^0_{QCD} - \bar{q}\mathscr{M}q$$

- In the massless case, the Lagrangian is invariant under separate unitary global transformations of left and right-hand quark fields, so-called *chiral rotations*
- To describe the strong interactions, it is necessary that the chiral symmetry is spontaneously broken: indeed, the chiral symmetry is not a symmetry of the ground state (no parity doublets).
- Chiral symmetry is also explicitly broken (quark mass $\neq 0$).

Modern nuclear forces: N3LO

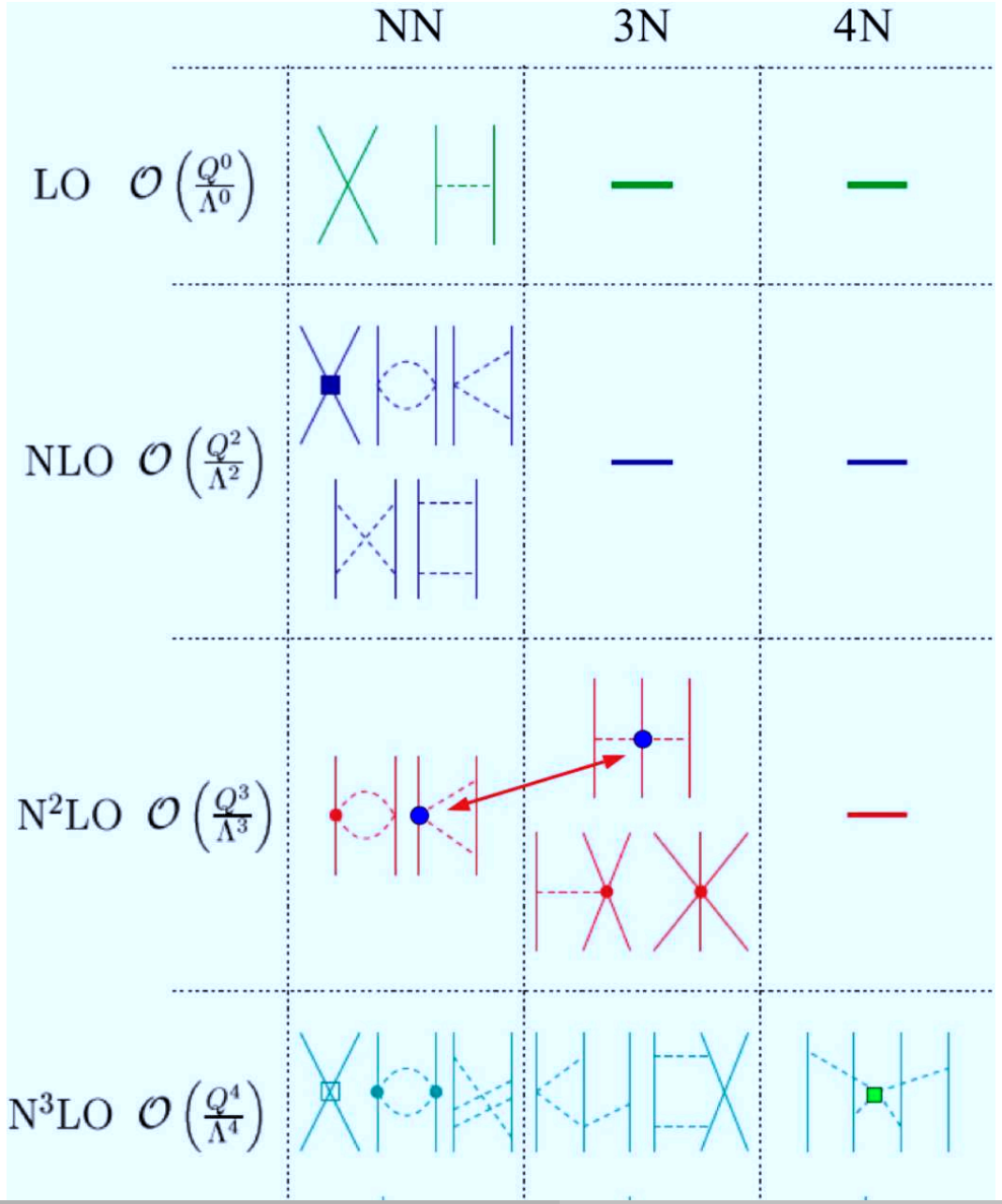

- We use pions and nucleons as degrees of freedom.
- The effective Lagrangian is classified using a systematic expansion based on a power counting in terms of $(Q/\Lambda_\chi)^\nu$, where ν is called chiral order and Λ_χ is the hard scale ($\sim$700MeV)
- ν=0 is called leading order, $\nu > 1$ are called next-to-$\nu - 1$ leading orders.
- Note hierarchy of nuclear forces.
- Coupling constants (LEC) adjusted to phase shifts and deuteron properties.

E. Epelbaum et al., Rev. Mod. Phys. 81 (2009) 1773.

Modern nuclear forces: N3LO

- The important role of 3N forces has been proven in light systems, e.g. in the no-core shell model calculations.

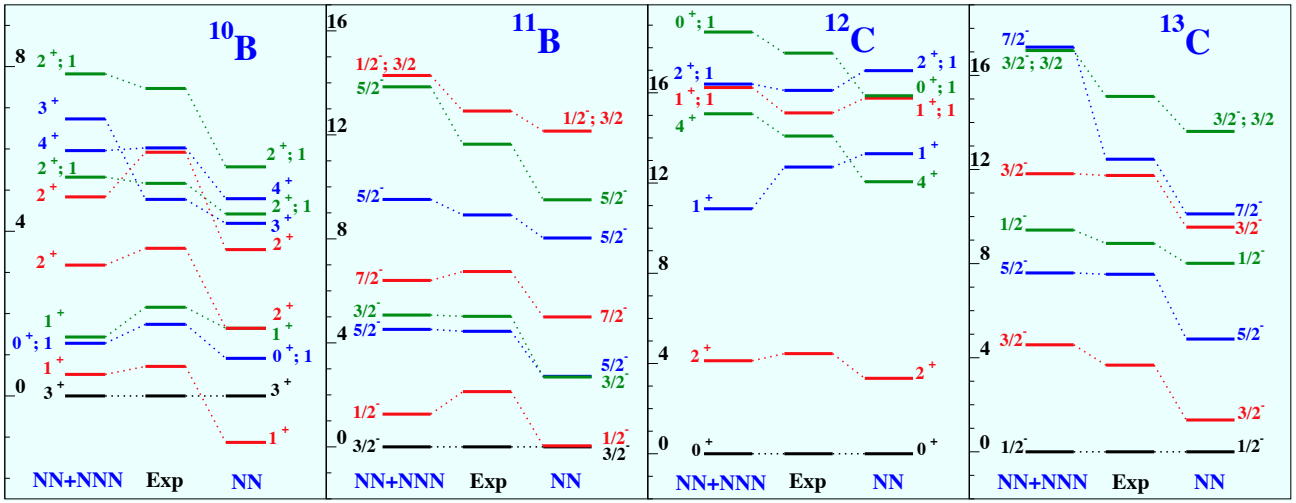

Excitation energies in light nuclei in NCSM with chiral EFT interactions. *P. Navratil et al., Phys. Rev. Lett. 99 (2007) 042501.*

- In heavier mass nuclei (shell model with the core) only 2-body interactions are nowadays calculated. The missing 3N part is taken into account by phenomenological corrections of TBME.
- Experimental information is crucial to constrain the interactions!

3N force from N2LO

$$V_{3N}^{(2\pi)} = \sum_{i\neq j\neq k} \frac{g_A^2}{8f_\pi^4} \frac{\vec{\sigma}_i \cdot \vec{q}_i \vec{\sigma}_j \cdot \vec{q}_j}{(\vec{q}_i^2 + m_\pi^2)(\vec{q}_j^2 + m_\pi^2)} F_{ijk}^{\alpha\beta} \tau_i^\alpha \tau_j^\beta$$

$$F_{ijk}^{\alpha\beta} = \delta_{\alpha\beta}(-4c_1 m_\pi^2 + 2c_3 \vec{q}_i \cdot \vec{q}_j) + c_4 \varepsilon^{\alpha\beta\gamma} \tau_k^\gamma \vec{\sigma}_k \cdot (\vec{q}_i \times \vec{q}_j)$$

$$V_{3N}^{1\pi} = -\sum_{i\neq j\neq k} \frac{g_A c_D}{8f_\pi^4 \Lambda_\chi} \frac{\vec{\sigma}_i \cdot \vec{q}_j}{\vec{q}_j^2 + m_\pi^2} \vec{\sigma}_i \cdot \vec{q}_i \vec{\tau}_i \cdot \vec{\tau}_j$$

$$V_{3N}^{ct} = \sum_{i\neq j\neq k} \frac{g_A c_E}{8f_\pi^4 \Lambda_\chi} \vec{\tau}_i \cdot \vec{\tau}_j$$

$g_A = 1.29, f_\pi = 92.4 MeV, \Lambda_\chi = 700 MeV, m_\pi = 138.04 Mev/c^2, \vec{q}_i = \vec{p}_i - \vec{p}_i'$

Soft-core potential V_{lowk} I

Separation of scales: Integrate out the high momenta and require that the effective interaction V_{lowk} reproduces the low-momentum scattering amplitude (calculated from V_{NN})

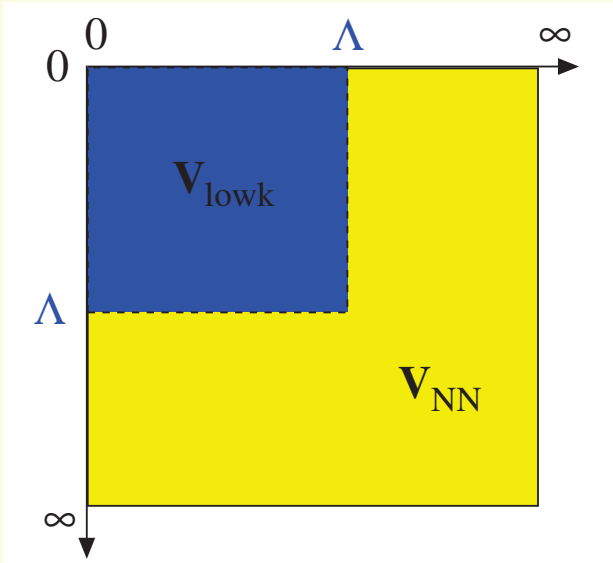

To obtain V_{lowk} potential we solve a RG flow equation in the momentum space:

$$\frac{d}{d\Lambda} V_{lowk}(k,k',\Lambda) = \frac{2}{\pi} \frac{V_{lowk}(k,k',\Lambda) T(\Lambda,k,\frac{\hbar^2\Lambda^2}{2m})}{1-(\frac{k}{\Lambda})^2}$$

starting from a given NN force V_{NN}, with the initial condition:

$$V_{lowk}(k,k';\Lambda) \longrightarrow_{\Lambda\to\infty} V_{NN}(k,k')$$

Calculation of the effective Hamiltonian

We know, that the realistic V_{NN} potential is not a good candidate for V in the perturbation theory. Thus we replace it with the G-matrix or V_{lowk}

$$V_{eff} = G + G\frac{Q}{E - H_0}V_{eff}$$

First-order

Second-order diagrams

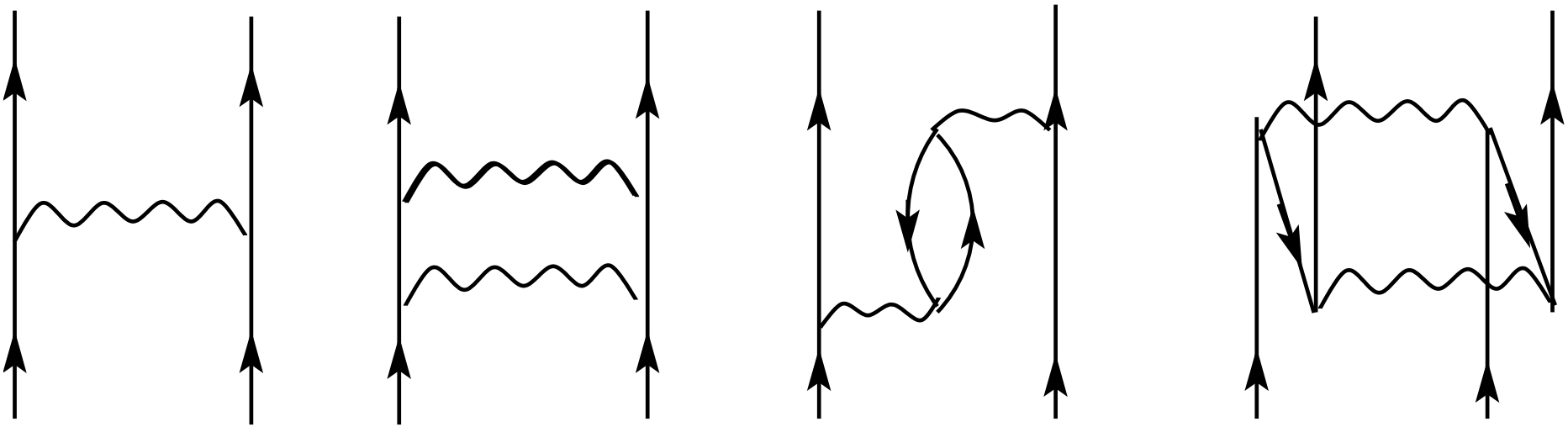

G-matrix

2p ladder

core-polarization

4p-2h

Beta-decay calculations

☞To calculate beta decay between two states one needs:

- accurate value of the decay energy ($T_{1/2} \sim \Delta E^{-5}$)
- matrix elements of Gamow-Teller ($\Delta J^{\pi} = 0^{+}, 1^{+}$) first forbidden ($\Delta J^{\pi} = 0^{-}, 1^{-}, 2^{-}$) transition operators

☞Nuclear model has to provide good description of masses, spectra and wave-functions

In r-process nuclei, GT is not enough, as protons and neutrons occupy different parity levels:

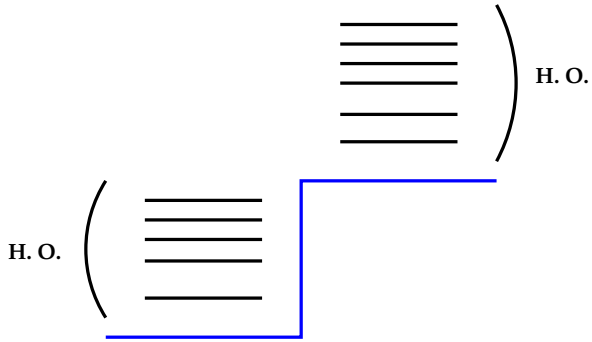

The beta half-life to a given state is gives as: $ft = 6146$, where the space phase factor f is given as

$$f = \int_1^{W_0} C(W) F(Z,W) (W^2-1)^{1/2} W (W_0 - W)^2 dW$$

For allowed transitions: $C(W) = B(F) + B(GT)$
For forbidden $C(W)$ is a function of the energy, and we have to calculate the integral

$$C(W) = k(1 + aW + \frac{b}{W} + cW^2)$$

Coeficients a,b,c

$$
\begin{aligned}
k &= \left[\zeta_0^2+\frac{1}{9}w^2\right]^{(0)}+\left[\zeta_1^2+\frac{1}{9}(x+u)^2-\frac{4}{9}\mu_1\gamma_1 u(x+u)\right. \\
&\quad \left.+\frac{1}{18}W_0^2(2x+u)^2-\frac{1}{18}\lambda_2(2x-u)^2\right]^{(1)}+\left[\frac{1}{12}z^2(W_0^2-\lambda_2)\right]^{(2)}, \\
ka &= \left[-\frac{4}{3}uY-\frac{1}{9}W_0(4x^2+5u^2)\right]^{(1)}-\left[\frac{1}{6}z^2W_0\right]^{(2)}, \\
kb &= \frac{2}{3}\mu_1\gamma_1\left\{-[\zeta_0 w]^{(0)}+[\zeta_1(x+u)]^{(1)}\right\}, \\
kc &= \frac{1}{18}\left[8u^2+(2x+u)^2+\lambda_2(2x-u)^2\right]^{(1)}+\frac{1}{12}\left[z^2(1+\lambda_2)\right]^{(2)}.
\end{aligned}
$$

Matrix elements

$$
\begin{aligned}
w &= -R^{\,A}F^0_{011} \\
&= \lambda\sqrt{3}\langle J_f T_f|||ir\,[C_1\times\boldsymbol{\sigma}]^0\,\boldsymbol{\tau}|||J_i T_i\rangle C, \\
x &= -\frac{1}{\sqrt{3}}R^{\,V}F^0_{110} \\
&= -\langle J_f T_f|||ir C_1\boldsymbol{\tau}|||J_i T_i\rangle C, \\
u &= -\sqrt{\frac{2}{3}}R^{\,A}F^0_{111} \\
&= \lambda\sqrt{2}\langle J_f T_f|||ir\,[C_1\times\boldsymbol{\sigma}]^1\,\boldsymbol{\tau}|||J_i T_i\rangle C, \\
z &= \frac{2}{\sqrt{3}}R^{\,A}F^0_{211} \\
&= -2\lambda\langle J_f T_f|||ir\,[C_1\times\boldsymbol{\sigma}]^2\,\boldsymbol{\tau}|||J_i T_i\rangle C, \\
w' &= -\frac{2}{3}R^{\,A}F^0_{011}(1,1,1,1) \\
&= \lambda\sqrt{3}\langle J_f T_f|||ir\,\frac{2}{3}I(1,1,1,1,r)\,[C_1\times\boldsymbol{\sigma}]^0\,\boldsymbol{\tau}|||J_i T_i\rangle C, \\
x' &= -\frac{2}{3\sqrt{3}}R^{\,V}F^0_{110}(1,1,1,1) \\
&= -\langle J_f T_f|||ir\,\frac{2}{3}I(1,1,1,1,r)C_1\boldsymbol{\tau}|||J_i T_i\rangle C, \\
u' &= -\frac{2\sqrt{2}}{3\sqrt{3}}R^{\,A}F^0_{111}(1,1,1,1) \\
&= \lambda\sqrt{2}\langle J_f T_f|||ir\,\frac{2}{3}I(1,1,1,1,r)\,[C_1\times\boldsymbol{\sigma}]^1\,\boldsymbol{\tau}|||J_i T_i\rangle C,
\end{aligned}
$$

Results: half-lives of r-process nuclei

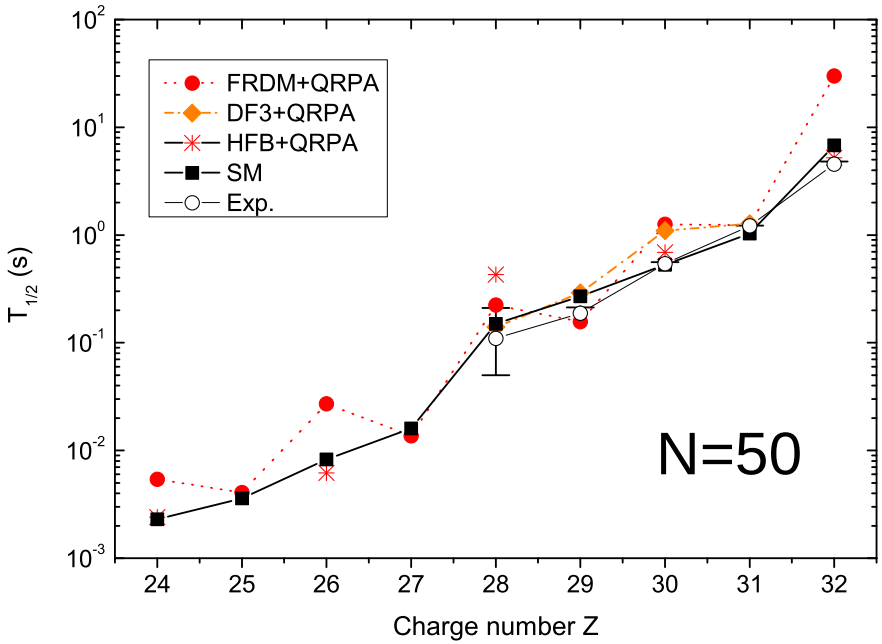

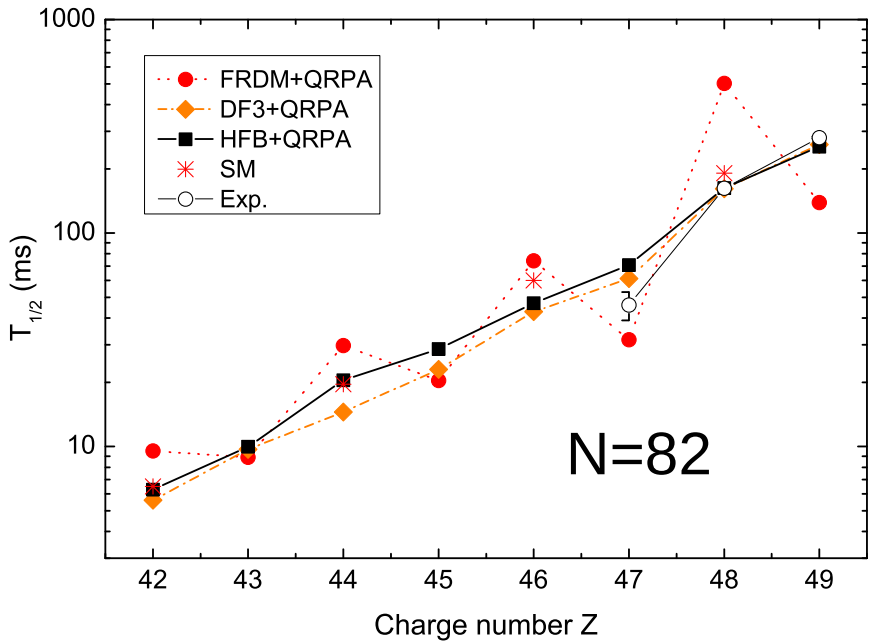

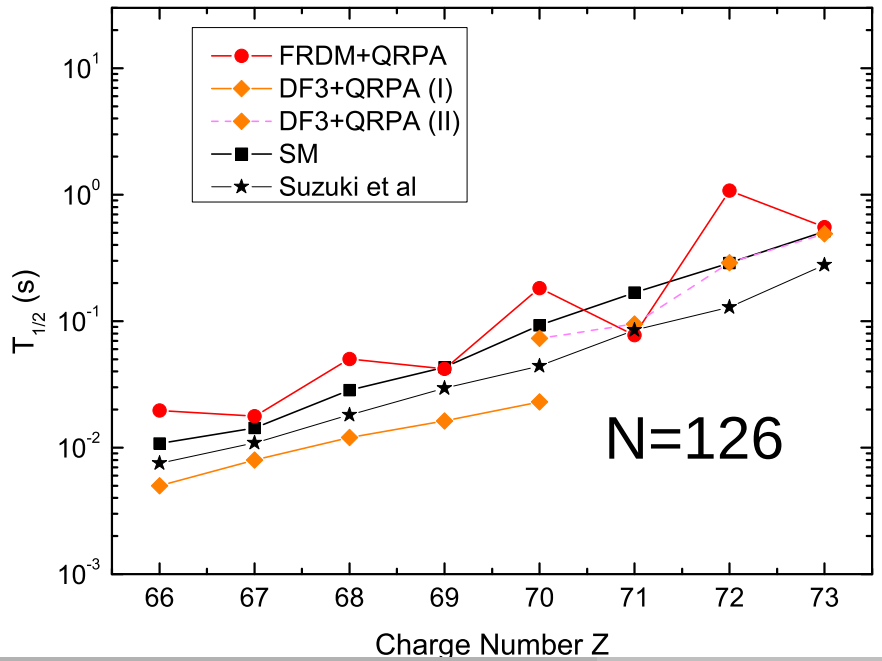

- Accurate description of Q_β, neutron emission probabilities and half-lives in the known region
- Universal quenching factors on GT and FF operators in all mass regions

Q. Zhi, J. Cuenca, E. Caurier, K. Langanke, G. Martinez-Pinedo, K. Sieja, Phys. Rev. C87 (2013) 025803

Lanczos strength function method

We can be interested in calculation of transition matrix elements $\langle \psi_f | \hat{O} | \psi_i \rangle$ to many final states.
For example in β-decay half-life calculation:

$$\lambda = \frac{ln2}{T_{1/2}} = \sum_f \lambda_f$$

$$\lambda_f = \frac{ln2}{K} f(Z, W_0)[B_f(F) + B_f(GT)]$$

To compute $B(GT)$ one needs:

- to determine the initial state $|\psi_i\rangle$
- find all possible final states $|\psi_f\rangle$
- compute all matrix elements $\langle \psi_i | M_{GT} | \psi_f \rangle$

The same holds for any other transition operator between states in the same nucleus:
M1, E1, E2...

or between different nuclei: GT, $\beta\beta$, $a^\dagger$, a, ...

Lanczos Strength Function

Let $\mathscr{O}$ be an operator acting on some initial state $|\Phi_{ini}\rangle$, we obtain the state $\mathscr{O}|\Phi_{ini}\rangle$ whose norm is the sum rule of the operator $\mathscr{O}$ in the initial state:

$$S = |\mathscr{O}|\Phi_{ini}\rangle| = \sqrt{\langle\Phi_{ini}|\mathscr{O}^2|\Phi_{ini}\rangle}$$

Depending on the nature of the operator $\mathscr{O}$,
the state $\mathscr{O}|\Phi_{ini}\rangle$ belongs to the same nucleus (if $\mathscr{O}$ is a e.m transition operator) or to another (Gamow-Teller, nucleon transfer, $a_j^\dagger/\tilde{a}_j$, $\beta\beta$, ...)

If the operator $\mathscr{O}$ does not commute with $\mathscr{H}$, $\mathscr{O}|\Phi_{ini}\rangle$ is not necessarily an eigenvector of the system BUT it can be developped in energy eigenstates:

$$\mathscr{O}|\Phi_{ini}\rangle = \sum_f S(E_f)|E_f\rangle \text{ and } \langle\Phi_{ini}|\mathscr{O}^2|\Phi_{ini}\rangle = \sum_f S^2(E_f)$$

with $\{S(E_f)\} = \{\langle E_f|\mathscr{O}|\Phi_{ini}\rangle\}$ being the strength function (or structure function)

Lanczos Structure Function

If we carry on the Lanczos procedure
using $|O\rangle = \mathscr{O}|\Phi_{ini}\rangle$ as initial pivot.
then H is again diagonalized to obtain the eigenvalues $|E_f\rangle$

U is the unitary matrix that diagonalizes $\mathscr{H}$ and gives the expression of the eigenvectors in terms of the Lanczos vectors:

$$U = \begin{array}{c} \\ |O\rangle \\ |2\rangle \\ |3\rangle \\ \vdots \\ \vdots \\ |N\rangle \end{array} \begin{pmatrix} |E_1 & |E_2\rangle & |E_3\rangle & \dots & |E_N\rangle \\ & & & & \\ & & & & \\ & & & & \\ & & & & \\ & & & & \end{pmatrix}$$

$$\tilde{S}(E_f) = U(1,f) = \langle E_f|O\rangle = \langle E_f|\mathscr{O}|\Phi_{ini}\rangle$$

How good is the Strength function $\tilde{S}$ obtained at iteration N compared to the exact one S?

Lanczos Structure Function

Any distribution can be characterized by the moments of the distribution.

$$\bar{E} = \langle O|H|O\rangle = \sum_i E_i |\langle E_i|\mathscr{O}|\Phi_{ini}\rangle|^2$$

$$m_n = \langle O|(H-\bar{E})^n|O\rangle = \sum_i (E_i-\bar{E})^n |\langle E_i|\mathscr{O}|\Phi_{ini}\rangle|^2$$

Gaussian distribution characterized by two moments ($\bar{E}, \sigma^2 = m_2$)

$g(E) = \frac{1}{\sigma\sqrt{2\pi}} \exp(-\frac{(E-\bar{E})^2}{2\sigma^2})$

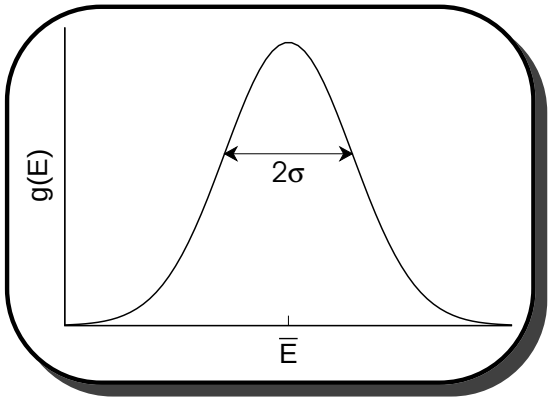

Lanczos Structure Function

Lanczos method provides a natural way of determining the basis $|\alpha\rangle$.

Initial vector $|\mathbf{1}\rangle = \frac{|O\rangle}{\sqrt{\langle O|O\rangle}}$

$$
\begin{aligned}
E_{12}|\mathbf{2}\rangle &= (H - E_{11})|\mathbf{1}\rangle \\
E_{23}|\mathbf{3}\rangle &= (H - E_{22})|\mathbf{2}\rangle - E_{12}|\mathbf{1}\rangle \\
&\dots \\
E_{NN+1}|\mathbf{N+1}\rangle &= (H - E_{NN})|\mathbf{N}\rangle \\
&\quad - E_{N-1N}|\mathbf{N-1}\rangle
\end{aligned}
$$

where

$$E_{NN} = \langle \mathbf{N}|H|\mathbf{N}\rangle, \quad E_{NN+1} = E_{N+1N}$$

Each Lanczos iteration gives information about two new moments of the distribution.

$$
\begin{aligned}
E_{11} &= \langle \mathbf{1}|H|\mathbf{1}\rangle = \bar{E} \\
E_{12}^2 &= \langle O|(H - E_{11})^2|O\rangle = m_2 \\
E_{22} &= \frac{m_3}{m_2} + \bar{E} \\
E_{23}^2 &= \frac{m_4}{m_2} - \frac{m_3^2}{m_2^2} - m_2
\end{aligned}
$$

Diagonalizing Lanczos matrix after N iterations gives an approximation to the distribution with the same lowest $2N$ moments.

Lanczos Structure Function

Initial vector $|\mathbf{1}\rangle = \frac{|\Omega\rangle}{\sqrt{\langle\Omega|\Omega\rangle}}$.

$$
\begin{aligned}
&E_{11} = \langle \mathbf{1}|H|\mathbf{1}\rangle \\
&E_{12}|\mathbf{2}\rangle = (H - E_{11})|\mathbf{1}\rangle \\
&E_{23}|\mathbf{3}\rangle = (H - E_{22})|\mathbf{2}\rangle - E_{12}|\mathbf{1}\rangle \\
&\dots \\
&E_{NN+1}|\mathbf{N+1}\rangle = (H - E_{NN})|\mathbf{N}\rangle \\
&\qquad\qquad\qquad\qquad -E_{N-1N}|\mathbf{N-1}\rangle
\end{aligned}
$$

where

$$E_{NN} = \langle \mathbf{N}|H|\mathbf{N}\rangle, \quad E_{NN+1} = E_{N+1N}$$

Each Lanczos iteration gives information about two new moments of the distribution.

$$
\begin{aligned}
&E_{11} = \langle \mathbf{1}|H|\mathbf{1}\rangle = m_1 = \bar{E} \\
&E_{12}^2 = \langle \mathbf{1}|(H - E_{11})^2|\mathbf{1}\rangle = m_2 \\
&E_{22} = \frac{m_3}{m_2} + \bar{E} \\
&E_{23}^2 = \frac{m_4}{m_2} - \frac{m_3^2}{m_2^2} - m_2
\end{aligned}
$$

$$
\begin{pmatrix}
E_{11} & E_{12} & 0 & 0 & 0 & 0 \\
E_{12} & E_{22} & E_{23} & 0 & 0 & 0 \\
0 & E_{32} & E_{33} & E_{34} & 0 & 0 \\
0 & 0 & E_{43} & E_{44} & E_{45} & 0 \\
 & & & & & \\
 & & & & &
\end{pmatrix}
$$